INVESTIGATION OF THE EFFECTS OF DRILLSTRING DYNAMICS TO MUD FLOW BEHAVIOUR

ARAVINDRAN A/L MUTHIAH

Mechanical Engineering

Universiti Teknologi PETRONAS

MAY 2015

INVESTIGATION OF THE EFFECTS OF DRILLSTRING DYNAMICS TO MUD FLOW BEHAVIOUR

PREPARED BY

ARAVINDRAN A/L MUTHIAH

17075

SUPERVISOR

DR TAMIRU ALEMU LEMMA

Mechanical Engineering

Universiti Teknologi PETRONAS

MAY 2015

INVESTIGATION OF THE EFFECT OF DRILLSTRING DYNAMICS TO MUD FLOW BEHAVIOUR

By

ARAVINDRAN A/L MUTHIAH
17075

A project dissertation submitted to the
Mechanical Engineering Programme
Universiti Teknologi PETRONAS
in partial fulfilment of the requirement for the

BACHELOR OF ENGINEERING (Hons)
(MECHANICAL)

Approved by,

_____

(DR TAMIRU ALEMU LEMMA)

UNIVERSITI TEKNOLOGI PETRONAS
TRONOH, PERAK
MAY 2015

CERTIFICATION OF ORGINALITY

This is to certify that I am responsible for the work submitted in this project, that the original work is my own except in the references and acknowledgements and that the original work contained herein have not been undertaken or done by unspecified sources or persons.

_____

ARAVINDRAN A/L MUTHIAH

ACKNOWLEDGEMENT

I wish to express my sincere gratitude to Department of Mechanical Engineering, for providing me with all the necessary facilities for the research especially the ANSYS CFX software. The license renewal is essential in order to ensure trouble free simulations and much helpful to complete the research on designated time frame.

I am also grateful to Dr. Tamiru Alemu Lemma, lecturer, in the Department of Mechanical Engineering who also my research supervisor. I am extremly thankful and indebted to him for sharing expertise, and sincere and valuable guidance and encouragement extended to me. I am trully appreciate his commitments and involvement in continous monitoring of research progress.

I take this opportunity to express gratitude to all of the Department faculty members for their help and support. I also thank my parents for the unceasin encouragement, support and attention. I also place on record, my sense of gratitude to one and all, who directly or indirectly, have lemt their hand in this venture.

ABSTRACT

The research deals with investigation of the effects of drillstring dynamics to mud flow behaviour. The drillstring motion and mud rheology have significant impact on pressure loss and cutting transport in drillstring. But this has not been explored for an Oil Based Mud (OBM) and other types of mud like Mixed Metal Hydroxide (MMH). The research will explore the pressure loss relationship among inlet velocity, eccentricity and rotational effect along inclination. The viscosity selection is based on Sisko's model which fits the viscous behaviour fairly for an Oil Based Mud. A part from that, the results of two benchmark cases from Nouar et al. (1998) and Escudier et al. (2002) have been validated by selecting Carbopol 940 (non-Newtonian) as drilling fluid and solved under ANSYS CFX before proceed with an actual case using Bentonite (B128) properties as an Oil Based Mud. Besides regular meshing techniques, Design of Experiment (DOE) is another solving method were used to determine the pressure gradient among inlet velocity, eccentricity and rotational. The input parameters such as inlet velocity, eccentricity and rotation were maintained from and Escudier et al. (2002). The results from DOE method shows that pressure gradient increases with inlet velocity but decreases linearly along pipe radius under eccentric condition and it well illustrated using 2D and 3D Response curve that haven been solved under Latin Hypercube sampling technique

.

Contents

CERTIFICATION OF ORGINALITY ii
ACKNOWLEDGEMENT iii
ABSTRACT iv
CHAPTER 1: INTRODUCTION 1
1.0 Background of study 1
1.1 Problem statement 2
1.2 Objective 3
1.3 Scope of study 3
CHAPTER 2: LITERATURE REVIEW 4
2.1 Fluid rheology 4
2.1.1 Bingham plastic model 4
2.1.2 Power law model 5
2.1.3 Hershel Buckley model 5
2.1.4 Modified Herschel Buckley model 6
2.1.5 Cross model 7
2.1.6 Sisko's model 8
2.1.7 Foams 8
2.2 Pressure loss and flow rate 9
2.3 Drill pipe rotation 10
2.4 Drill Pipe eccentricity 12
2.5 Computational Fluid Dynamic (CFD) Analysis 12
CHAPTER 3: METHODOLOGY 14
3.1 Literature review 14
3.2 Computational Fluid Dynamics (CFD) analysis 14
3.2.1 Benchmark problem 14
3.2.2 Modelling and simulation of case study 14
3.2.3 Parametric study and comparison 14

3.2.4 Results discussion and documentation 14

CHAPTER 4: RESULTS AND DISCUSSIONS 18

4.1 Introduction 18

4.2 Case-1: Hershel Buckley Fluid model (Nour et al, 1998) 18

4.2.1 Axial Velocity profile curves 20

4.2.2 Tangential Velocity Curves 23

4.3 Case-2: Cross model (Escudier et al, 2002) 25

4.3.1 Axial velocity profiles at, $\epsilon = 0.8$ 27

4.3.2 Tangential velocity profiles at, $\epsilon = 0.8$ 29

4.4 Pressure gradient using Design on Experiment (DOE) method 33

4.5 Oil Based Mud (OBM) flow behaviour using Sisko's model 38

CHAPTER 5: CONCLUSION AND RECOMMENDATION 43

5.1 Conclusion 43

REFERENCES 44

APPENDICES 46

LIST OF FIGURES

Figure 1	Fluid Rheological Model …….....	5
Figure 2	Effect of pipe rotation at 40 L/s……...	10
Figure 3	Annular grid structure …….....	11
Figure 4	Simulation methodology flowchart……..	15
Figure 5	Gantt chart (FYP I)……	16
Figure 6	Gantt chart (FYP II)…….....	17
Figure 7	Annular geometry…….....	19
Figure 8	Concentric annular pipe…….....	19
Figure 9	Plot for pressure gradient…….	55
Figure 10	Plot for pressure gradient…….	58
Figure 4.1	(a): Inlet velocity, u = 0.0740 m/s, ω (rad/s) = 0……..... .21	
Figure 4.1	(b): Inlet velocity, u = 0.0728 m/s, ω (rad/s) = 13.8…….....22	
Figure 4.1	(c): Inlet velocity, u = 0.0728 m/s, ω (rad/s) = 28.1…….. …22	
Figure 4.1	(d): Inlet velocity, u = 0.0728 m/s, ω (rad/s) =2.78……..... 23	
Figure 4.1	(e): Inlet velocity, u = 0.0728 m/s, ω (rad/s) =14.00…….. 23	
Figure 4.1	(f): Inlet velocity, u = 0 m/s, ω (rad/s) =13……. …24	
Figure 4.2	(a): Ta: 3500, Re: 241, U: 0.268 m/s, ω: 5.24 rad/s…… …28	
Figure 4.2	(b): Ta: 3500, Re: 241, U: 0.268 m/s, ω: 5.24 rad/s……28	
Figure 4.2	(c): Ta: 3500, Re: 241, U: 0.268 m/s, ω: 5.24 rad/s……29	
Figure 4.2	(d): Ta: 3500, Re: 241, U: 0.268 m/s, ω: 5.24 rad/s…….. ..29	
Figure 4.2	(e): Ta: 3172, Re: 241, U: 0.268 m/s, ω: 5.35 rad/s…… 30	
Figure 4.2	(f): Ta: 3172, Re: 241, U: 0.268 m/s, ω: 5.35 rad/s…….. ..30	
Figure 4.2	(g): Ta: 3172, Re: 241, U: 0.268 m/s, ω: 5.35 rad/s……. 31	
Figure 4.2	(h): Ta: 3172, Re: 241, U: 0.268 m/s, ω: 5.35 rad/s…….. ..31	

LIST OF TABLES

Table 1 : Experimental data by Nouar et.al (1998) …….6

Table 2 : Experimental data by Escudier et.al (2002)……..8

Table 3 : Experimental data by Sun et.al (2013)…….12

Table 4 : Parameter data by Nouar et.al (1998)……..19

Table 5 : CFX Mesh Parameter……...20

Table 6 : Parameter data by Escudier et al (2002)……...25

Table 7 : Pipe radius dimensions for Sector A, B, C&D…….27

Table 8 : Parametric values of DOE ……32

Table 9 : Design of Experiment (DOE) point…….38

CHAPTER 1: INTRODUCTION

1.0 Background of study

The drill string is an important component at rotary drilling process. It is the connection between rig and the drill bit. Drill string is an assembled collection of drill pipe, drill collars and drill bit. When the drilling process takes place, a special drilling mud is used to cool the bit and carry the rock cuttings back to the surface thru annuli (clearance between drill pipe and casing).

Extensive drilling process at complex well structure require a critical study on cutting transport parameters. According Sun et al. (2014), it is important to study critical parameters that affects the cuttings behaviour. It finds significant impact on the mud pump flow rate which transport the mixture of cuttings and mud from annuli back to mud tank and vice versa. Critical parameters here refers to pressure loss, rotating inlet, velocity inlet, and eccentricity.

The drill pipe rotations have significant impact between mud flow behaviours and annular velocities. A study from Sifferman et al. (1974), found that annular velocity and fluid rheological properties are the most important factors influencing the transportability of a fluid and other variables such as particle size, drill pipe rotation, and drill pipe eccentricity have only moderate effects on cuttings carrying capacity.

Types of mud have significant impact on carrying the cuttings back to well head. Water based mud (WBM) are most primarily used in drilling rather than Oil Based Mud (OBM) but it possessed some interesting properties such as provides good lubrication with higher boiling points (Khodja et al, 2010). All oil muds consist mixture of organoclay (OC) with mineral oil that used for minimum pressure losses and low permeability reservoirs.

Inlet velocity is another parameter mentioned by Ikoku (1986) who used an approach to develop a procedure for the determination of the minimum velocity foam injection at well head and from the results explained about fluid

velocity at the bottom should be at least 10% higher than terminal velocity at same depth to get an effective cutting transport.

The drill pipe eccentricity is important in calculating the carrying capacity by manipulating the flow rate of drilling fluid in the lower side of the eccentric annulus for an effective cutting transport which highlighted by Luo and Penden (1987) on study effect of the pipe hole eccentricity on cutting transport. Power law and Bingham plastic are two common rheological model used to investigate the cutting transport behaviour for the past extensive research.

The drillstring motion and mud rheology have significant impact on pressure loss and cutting transport in drillstring. But this has not been explored for an Oil Based Mud (OBM) and other types of mud like Mixed Metal Hydroxide (MMH). The research will explore the pressure loss relationship among inlet velocity, eccentricity and rotational effect along inclination. The research will explore the pressure loss relationship among inlet velocity, eccentricity and rotational effect along inclination.

1.1 Problem statement

Drillstring motion and mud rheology affects the pressure loss and cutting transport in the drillstring. This is not been studied or explored for Oil based mud (OBM) and other types of mud like Mixed Metal Hydroxide (MMH).

The mud flow behaviour for Oil base mud (OBM) type will be analysed using Sisko's model which emphasize on rheological properties. The model includes density and viscosity parameters which the author believes have effects on transport efficiency due flow rate and pipe rotations.

In addition, the author would to investigate another parameter of study called as eccentricity. The analysis need to come with an outcomes on how the drill pipe eccentricity along drill pipe rotation could affects the Oil based Mud (OBM) flow behaviour at inclination.

The situation is idealised as steady, isothermal, fully developed laminar flow of generalised Non-Newtonian fluid through an annulus consisting with an outer cylinder and inner cylinder which may offset (i.e eccentric) and rotating. The governing equation such as continuity, axial momentum, tangential momentum, radial momentum with boundary condition of inner and outer cylinder.

1.2 Objective

The objectives of research as following:

a) To model drillpipe geometry and investigate the mud flow behaviour in drillstring using ANSYS CFX software

b) To investigate the relationship among pressure loss, rotational effects, inlet velocity along rotation and inclination using Oil based Mud (OBM) type.

c) To investigate the effect of eccentricity at drillstring on mud flow behaviour.

1.3 Scope of study

The scope of the research are limited as following:

a) Selection of drillstring to be decided based on hydraulic length of non-Newtonian fluid.

b) Settings for inlet velocity, rotation and eccentricity to be decided using Design of Experiment (DOE) method.

c) Mud rheology based on Oil Based Mud (OBM) and other type mud under consideration are Mixed Metal Hydroxide (MMH)

d) The viscosity selection for and Oil based Mud (OBM) based on Sisko's Model

CHAPTER 2: LITERATURE REVIEW

2.1 Fluid rheology

One of the primary functions of the drilling fluid is to make an efficient transportation of cuttings to the surface. It depends on fluid velocity and fluid rheological model which provides the characteristic of the fluid itself. Fluid are characterized into two which are Newtonian and non-Newtonian fluid. Non Newtonian rheological models are Bingham plastic, API, and Herschel Buckley. The research will focusing on improved Herschel Buckley model o transport behaviour. Following are typical rheological behaviour with shear stress against shear rate;

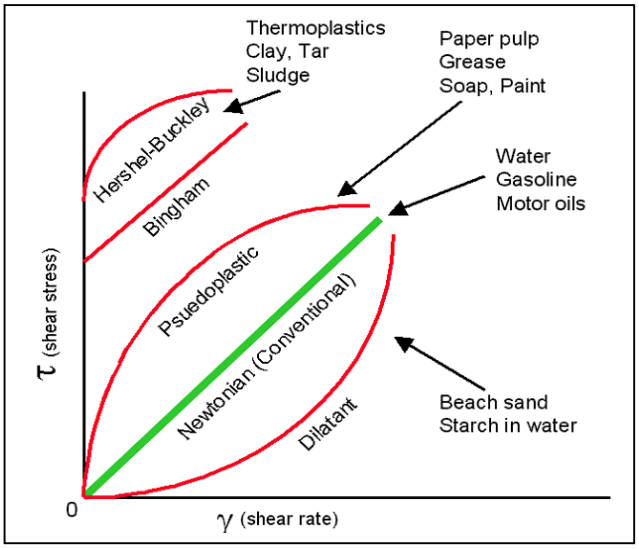

Figure 1: Fluid Rheological model

2.1.1 Bingham plastic model

The shear-shear rate is a linear relationship and slope represents the Bingham plastic. The intercept is the yield stress of the fluid. To initiate flow, a minimum pressure is required to overcome the yield stress (Bourgoyne et al, 1991). The model is given as

$$\tau = \mu\rho\gamma + \tau_Y$$

The Bingham plastic model is the standard viscosity model used which can fit high shear rate viscosity data reasonably well. **μp** (plastic viscosity) is

generally associated viscosity of base fluid, size and shape of solids in slurry. The yield stress is associated with tendency of the components to build a shear resistant.

2.1.2 Power law model

This rheological model referred as Ostwald-de Walle model. Similar to Bingham plastic model, this model requires two parameters: the consistency (K) and the flow behaviour index (n) for fluid characterization. The power law is defined:

$$\tau = K\gamma^n$$

This can be used to represent pseudo plastic fluid (n < 1), a Newtonian fluid (n=1) and a dilatant fluid (n>1). Therefore, the deviation of the dimensionless flow behaviour index (n) from unity characterizes the degrees to which the fluid behaviour is non Newtonian. In addition, the power law model equation only valid for laminar flow regime; thus the low shear rate (Bourgoyne et al, 1991).

2.1.3 Hershel Buckley model

Hershel Buckley equation is preferred instead of power law and Bingham plastic model because it results more accurate model of rheological behaviour (Hemphill et al, 1993). Following is expression for the equations

$$\tau = \tau_0 + k(\dot{\gamma})^n$$

There is been research conducted by Kelessidis et al (2006) impact of pressure drop, velocity profiles and penetration rates during drilling using Hershel Buckley model. The chosen flow is laminar and it significantly affects the pressure drop velocity profiles in concentric annulus and pipes according to rheological parameters.

In research done by Kelessidis et al, (2006) insist the results outcomes have demonstrated that, it is very crucial to make the best simulations of rheological behaviour of drilling fluids before computing hydraulic parameters. This could avoid problems during drilling operations of existing drilling fluids. Following describes the experiment data investigation

conducted by Nouar.et al (1998) using Carbopol as drilling fluid with Hershel Buckley rheological model.

Table 1: Experimental data (Nouar et.al, 1998)

No	Benchmark parameter	Type/Values	Unit
1	Drilling fluid	Carbopol	
2	Drilling fluid density (ρ)	940	kg/m3,
3	Eccentricity	0	
4	Fluid Rheological Model	Hershel Buckley	
5	Pipe inner diameter(d_i)	40	mm
6	Pipe outer diameter (d_o)	65	mm
7	Pipe length (L)	165	mm

2.1.4 Modified Herschel Buckley model

Mendes and Dutra, 2004 have conduct an investigation on viscosity function for viscoplastic liquids for highly shear thinning such as pastes and slurries is proposed. The original model of Herschel Buckley model used was as following:

$$\tau = \tau_{0} + k(\gamma)^{n}$$

However, Mendes and Dutra, 2004 have discovered the original equation shear rate tend to be very low. They have come up with modified equation which gives following expression;

$$\tau = (1 - \exp\left(-\frac{\eta_0 \gamma}{\tau_0}\right))(\tau_0 + k\gamma^n)$$

The zero shear rate viscosity is just equal to the ratio τ/γ provided τ is small enough than τ_0 to ensure that γ is within the zero shear rate plateau region. The behaviour index η is the slope power law region.

2.1.5 Cross model

Escudier et.al (2002) have conduct an experimental investigation on fully developed laminar flow of non – Newtonian liquids at 80% concentric annuli with and without centre body rotation using Cross model. The workingfluid was an aqueous solution of 0.1% xanthan gum and 0.1% caboxymethylcellulose (CMC).

Escudier et.al (2002) present the results of an extensive series of calculations for power law fluids. At the same time, they had developed a general methodology for fluids that obeying other viscosity models such as Cross model and Herschel Buckley model.

Following table shows the parameter used by Escudier et.al (2002) to conduct the experiment:

Table 2: Experimental data by Escudier et.al (2002)

Parameter	Data	Unit
Fluid type	0.1% Xanthan gum, 0.1% (CMC)	
Density	940	kg/m^3
Reference fluid model	Power law and Herschel Buckley	
Flow type	Laminar	
Fluid model	Cross model	
Max flow rate	0.025	m^3/s
Pipe length	5.775	m
hydraulic diameter ratio	116	
Max rotation	126	rpm
Eccentricity	0.8	

Nouar et al. (1998) have conducted similar experiment under laminar flow but the working fluid is 0.2% Carbopool with a density of $940kg/m^3$ for a concentric and eccentric annulus with centre body rotation.

Hence, Escudier et.al (2002) improved the experimental data of Nouar et al (2002) by adding new data which doubles the database and emphasize highly eccentric (80%) situation and do some comparison regarding on results

obtained. The expression for the cross model used in the experiment are as following;

$$\frac{\mu_0 - \mu_\infty}{\mu - \mu_\infty} = 1 + K_{CR}\gamma n_{cr}$$

The values for the consistency index K_{CR} and the exponent n_{cr} are listed in appendices for references.

2.1.6 Sisko's model

It is one of the rarely used rheological models to describe the behaviour of drilling fluids to perform hydraulic calculations in the oil and gas industry. This is because the form of this model makes the derivation of tractable expressions for pressure drop as a function of flow rate nontrivial or impossible (Bailey and Peden, 2000). The solution of their expression required rigorous computation. The constitutive law is expressed in equation below.

$$\eta = \eta_{\infty 0} + k_0 \dot{\gamma}^{\eta_0 - 1}$$

Weir and Bailey (1996) statistically investigated twenty different rheological models on four different types of drilling fluid. After ranking of the models, Sisko model was selected as overall best fit for the selected fluids. They continued to derive a generalized consistent pressure loss equation which is independent on the type of rheological model for flow of fluids in a pipe and concentric annulus during laminar flow regime.

2.1.7 Foams

Foam is another types of drilling fluid commonly used to underbalanced drilling because of its low variable density which makes an adjustment in foam density to control on bottom hole pressure. Foam fluids generally consist of 5-25% of the liquid phase and 75-95% of the gaseous phase.

Rooki et.al (2015) have conducted a CFD simulation on rheological model effect on cuttings transport. The working fluid for this simulation is foams. Herschel Buckley and Power law are two rheological models used to study effect of cutting transport in concentric and eccentric annulus during foam drill operations. Rooki et al (2015) have distinguish the foam properties based on

density and quality. Below shows the equations for quality and density parameter;

$$\Gamma = \frac{V_g}{V_g + V_l} \, X \, 100$$

Where Γ the foam quality (%), Vg is is the gas volume and V_l is the liquid volume. The foam quality ranges between 0 to1 depending on the amount of gas in the foam. When the gas flow rate increase, the foam quality will increase too which eventually increase the viscosity and decrease the density.

$$\rho_f = \Gamma \rho_g + (1 - \Gamma)\rho_l$$

Where ρ_f is the foam density; ρ_g represents the gas density; ρ_l is known as liquid density. When there is change on gas volume, it affect change on pressure and temperature which resulting change in foam density.

In addition, Rooki et al (2015) also discuss the importance of foam rheological behaviour to determine the efficiency of cutting transport in drilling operations. There are certain disagreement on foam model selection due to difference in analytical approach, experimental setup and types of foaming agent. Rooki et al (2015) have decided to express the flow behaviour using Bingham plastic and Herschel Buckley model.

2.2 Pressure loss and flow rate

Keeping down hole pressure in control is important in any drilling situation. The pressure losses mostly occur during mud circulation as a function of flow rate. Therefore, it is crucial to study on pressure drop and flow rate profile of drilling mud in drill string and annulus in order to optimize the pump power to extend the drilling operations and at the same time contributes towards effective cutting transport to the surface.

Udo and Okon (2013) have conduct research on pressure drop-flow rate profile of some locally formulating drilling fluids: water based were evaluated in different flow regime in drill pipe and annulus using Bingham plastic and Power law rheological models. The outcomes from their study shows that

Power law models best described the rheology of the formulated synthetic based drilling fluid under turbulent flow.

Power law models results in high pressure loss when compared to Bingham plastic model in drill pipe and vice versa in the annulus. However in laminar flow condition, the Bingham plastic model results in high pressure drop compared with power model in both drill pipe and annulus.

Sun et al (2014) have conduct an experiment o effects of drill pipe rotation on cuttings transport using CFD analysis in complex structure wells. The results expressed in graphical form as following;

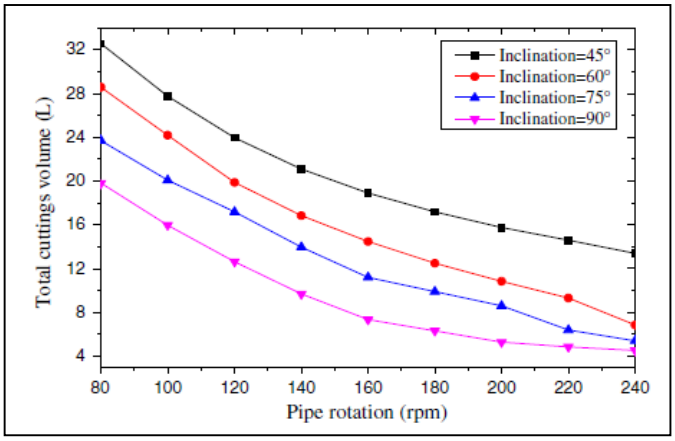

Figure 2: Effect of pipe rotation at flow rate (40L/s)

The graph indicates pressure drop at various inclination angles when the rotation of drill pipe increase significantly between 80-100 rpm. The data discussed only for 40 l/s flow rate and these have been tested for 30 and 50 L/s of flow rate and gave the same results as well.

2.3 Drill pipe rotation

Sanchez et.al (1999) states that smaller cuttings are more difficult to transport. But if there is increase in rotary speed with high viscosity muds, the smaller cuttings seems to easier to transport. Generally, in inclined wells, low viscosity muds clean better than high viscosity muds but depending upon cutting size, viscosity and rotary speed level.

Similarly, Sun et.al (2013) have published a journal on effect of drill pipe rotations on cutting transport using Computational Fluid Dynamics analysis (CFD) in complex structure wells. The analysis were carried out under different flow rates (30 L/s – 50 L/s), pipe rotation varies from 80 rpm – 240 rpm with four different inclinations (45º, 60º, 75º and 90º).

The CFD results indicates pipe rotation has significant effect on distribution of annular cuttings along the cutting transport at low and medium flow rates. However, there is no additional contribution of pipe rotation after reaching critical speed at high flow rates. Buckingham-π theorem and least square method were used to estimate cuttings concentration and annular pressure drop.

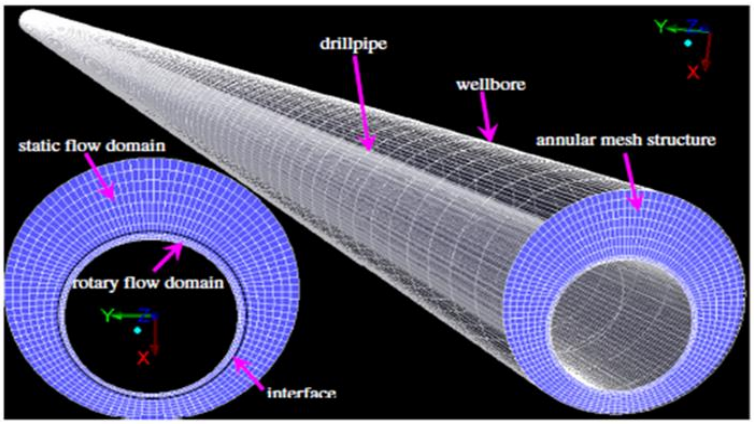

Figure 3: Annular grid structure

Table 3: Experimental parameter

Testing Parameter	**Values**	**Unit**
Drilling fluid density (ρ)	1200	Kg/m^3
Drilling fluid viscosity (μ)	30	mPa.s
Cutting density (ρ)	2500	Kg/m^3
Cutting diameter (D)	8	mm
Drill pipe length	12	m
Drill pipe diameter	127	mm
Eccentricity	0.5	
Drill pipe rotation	80-240	Rpm
Flow rate	30-50	L/s
Fluid model	Power Law	

2.4 Drill Pipe eccentricity

Drill pipe eccentricity is a crucial analysis in vertical wells. Iyoho and Azhar (1981) approach the problem by using bipolar coordinates to define the eccentric annular geometry and developed methods for velocity profile calculations which involve extensive numerical iterative computations using Power law fluids. But the results produced were unrealistic symmetric velocity and linear shear stress profile.

Luo and Peden (1987) use two common rheological models which are Power law and Bingham plastic models to define the rheological behaviour of the drilling fluids. From the analysis, the effect of pipe eccentricity on cutting transport is been evaluated. The author came up with an equation to calculate the radius at which the velocity is maximum and shear stress is zero in eccentric annulus for non-Newtonian fluid using power law and Bingham plastic models.

The eccentricity have some effects on drill pipe rotations. Richard et al (1989) states that when particle velocity increases, it will affected by rotary speed at low annular flow rates and at low level eccentricity. But soon as eccentricity increases, the effects of rotary speed variation decreases. When the flow rate is high and low level eccentricity, the effect was almost negligible.

2.5 Computational Fluid Dynamic (CFD) Analysis

The usage of CFD is more proven in many areas of fluid flow. ANSYS CFX is the CFD software model application provides opportunity for researchers to investigate on more complex problems. The requirements of the research is to do model frame of a drill pipe with specific length and diameter input. Basically, the analysis will be on incompressible two phase flow. The drilling fluids will be represented by Power law and Bingham plastic model.

The desired drill pipe geometry will be represent by mesh volumes. There are certain boundary condition will be set before starting the analysis such as flow condition (laminar or turbulent), conservation of mass and momentum equation but the no energy since the pipe condition is under isothermal. Hence, no temperature parameter will be evaluated.

i) Axial momentum

$$\rho\left(w\frac{\partial u}{\partial r}+\frac{v}{r}\frac{\partial u}{\partial \phi}\right)=\frac{\partial \rho}{\partial z}+\frac{1}{r}\frac{\partial}{\partial r}\left(\mu r\frac{\partial u}{\partial r}\right)+\frac{1}{r^2}\frac{\partial}{\partial \phi}\left(\mu\frac{\partial u}{r\,\partial \phi}\right)$$

ii) Tangential momentum

$$\rho\left(w\frac{\partial v}{\partial r}+\frac{v}{r}\frac{\partial v}{\partial \phi}+\frac{wv}{r}\right)$$
$$=\frac{1}{r}\frac{\partial \rho}{\partial \phi}+\frac{1}{r^2}\frac{\partial}{\partial r}\left[\mu r^3\frac{\partial}{\partial r}\left(\frac{v}{r}\right)+\mu r\frac{\partial w}{d\phi}\right]+\frac{2}{r}\frac{\partial}{\partial \phi}\left(\frac{\mu}{r}\frac{\partial v}{\partial \phi}+\frac{\mu w}{r}\right)$$

iii) Radial momentum

$$\left(w\frac{\partial w}{\partial r}+\frac{v}{r}\frac{\partial w}{\partial \phi}-\frac{v^2}{r}\right)$$
$$=\frac{\partial p}{\partial r}+\frac{2}{r}\frac{\partial}{\partial r}\left(\mu r\frac{\partial w}{\partial r}\right)+\frac{\partial}{\partial \phi}\left[\mu\frac{\partial}{\partial r}\left(\frac{v}{r}\right)\right]+\frac{1}{r^2}\frac{\partial}{\partial \phi}\left(\mu\frac{\partial w}{\partial \phi}\right)$$

Bilgesu et.al (2002) have previously had previously use Computational Fluid Dynamics (CFD) as a tool to study the cutting transport at wellbores. The author have successfully investigate how annular velocities, mud flow rates and mud densities could affects the cutting transport efficiency ranging from different inclination angles by using CFD analysis at well bore. The same approach will be used for current analysis but at drill pipe.

CHAPTER 3: METHODOLOGY

3.1 Literature review

The analysis mainly on sinusoidal vibration motion effect at drill string during cutting transport in deep-water drilling. To be precise, the author would like to study the effects at drill pipe which eventually affects the cutting transport efficiency. Resources like journals, books and articles from internet have been very helpful as a supporting statement for the literature review.

3.2 Computational Fluid Dynamics (CFD) analysis

The analysis involve modelling and simulation using ANSYS CFX. The drill pipe geometry will be analyse in the form of mesh grid.

3.2.1 Benchmark problem

- Perform analysis with simple case study using Power law models or Hershel Buckley model itself for trial purpose.
- Validate the analysis for different case studies.
- Perform mesh independence study.

3.2.2 Modelling and simulation of case study

- Drill pipe geometry (length and diameter) and annular cuttings modelling
- Model and simulate using Hershel Buckley model
- Validate the analysis through successive simulations

3.2.3 Parametric study and comparison

- Investigate the effects of mud flow rate and drilling fluid rheological properties on cutting transport efficiency at drill pipe.

3.2.4 Results discussion and documentation

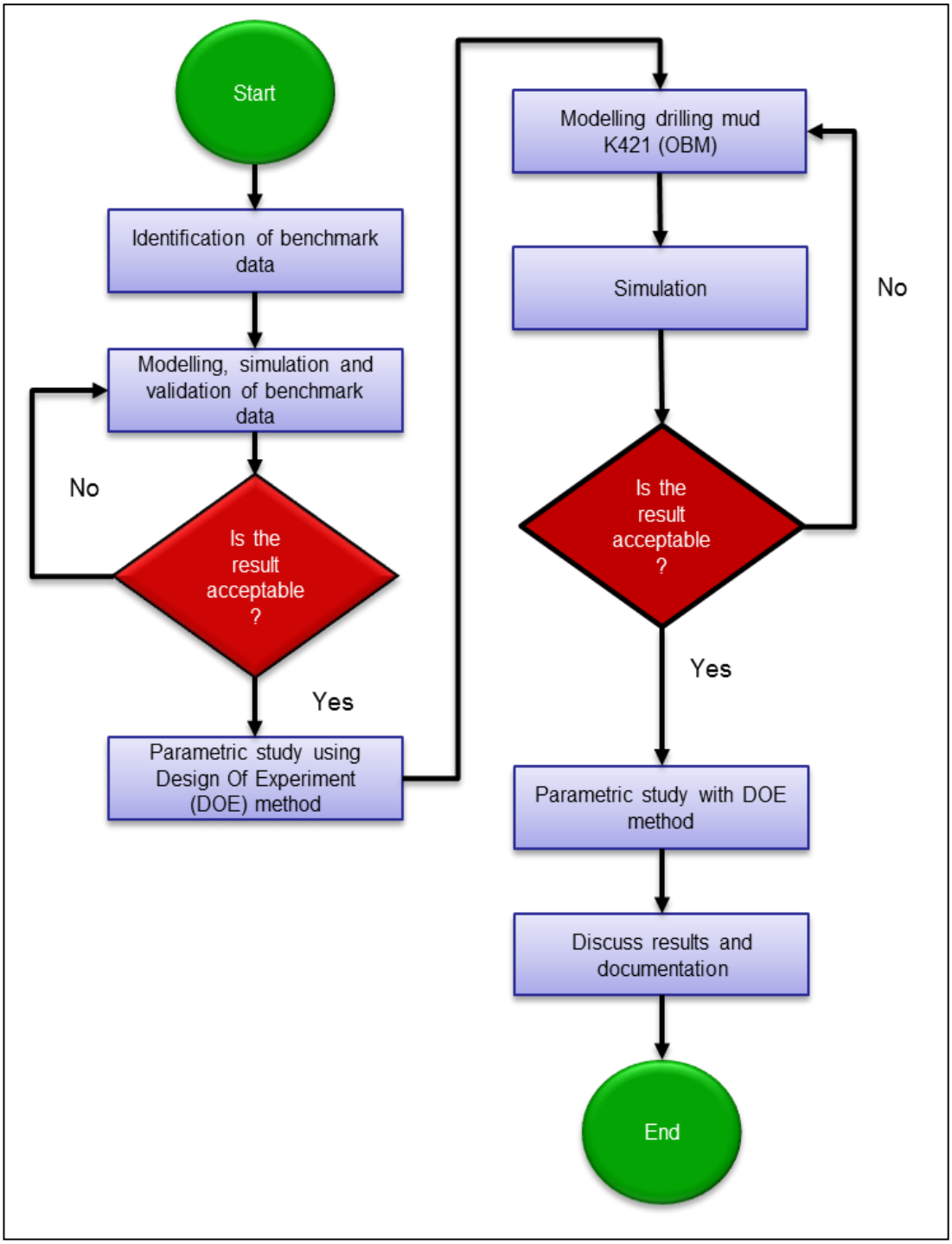

Figure 4: Simulation methodology flowchart

No	Activities / week	1	2	3	4	5	6	7	8	9	10	11	12	13	14
1	**Title selection**														
2	**Weekly meeting with Supervisor**														
3	**Literature review study**														
4	**Extended proposal submission**														
5	**AANSYS software study (LAB)**														
6	**Proposal defence**														
7	**Benchmark problem (trial case study)**														
	i) Creating the geometry														
	ii) Meshing														
	iii) First trial test														
	iv) Analysis and discussion														
8	Interim report submission														

In progress **Supervisor meeting** **Submissions**

Figure 5: Gantt chart (FYP I)

No	Activities / week	1	2	3	4	5	6	7	8	9	10	11	12	13	14
1	**Benchmark problem (research base)**														
	i) creating geometry														
	ii) Meshing														
	iii) Verify geometry viscosity model														
	iv) Simulate mesh using Hershely Berkely model														
	v) Simulate for validation														
	vi) Analysis and discussion														
	Weekly meeting with Supervisor														
2	**PRE SEDEX**														
3	**Submission of dissertation (soft copy)**														
4	**Submission of technical paper**														
5	**Viva**														
6	**Dissertation submision (Hard bound & CD)**														

In progress **Supervisor review** **Submission**

Figure 6: Gantt chart (FYP II)

Table 4: Research milestone

Milestone	Date
Finalize the selection of benchmark problem	26/02/2015
Complete simulation of Benchmark problem (for different case)	20/03/2015
Simulations of case s problem	26/06/2015
Completion of parametric study with results validity	23/07/2015

CHAPTER 4: RESULTS AND DISCUSSIONS

4.1 Introduction

The research focus on two close references from Nouar et al. (1998) and Escudier et al. (2002) as a benchmark analysis. Nouar et al. (1998, approach on velocity distribution for the laminar flow on non-Newtonian fluid through an annulus. The experimental investigation provides the in depth measurements of 0.2% Carbopol for a concentric annulus with centre body rotation using Herschel Buckley as general rheological model.

While Escudier et al. (2002) provide and extensive series of calculations for power law fluid. A general methodology have been developed where the power law results can be applied to flows for fluid obeying other viscosity model like Herschel Bukley, Carreau and Cross. Escudier et al. (2002) emphasize more on highly eccentric condition (80

4.2 Case-1: Hershel Buckley Fluid model (Nour et al, 1998)

Based on literature review study, the author have decided to conduct numerical data analysis using CFD and make comparison with previous research data provided by Nouar et al (1998) as a benchmark analysis. Following table shows the parameter used by Nouar et al (1998) in conducting investigation on concentric annulus with centre body rotation using 0.2% Carbopol, density $\rho =$ 940kg/m3, eccentricity $\epsilon = 0$, and $\kappa = 0.615$. The rheological model used was Herschel Buckley model.

Table 5: Experimental investigation by Nouar et al (1998)

U (m/s)	**ω (rad/s)**	$\boldsymbol{\tau_y}$ **(Pa)**	$\boldsymbol{K_{HB}}$	$\boldsymbol{n_{HB}}$	**Re**
0.0740	0	26.54	20.93	0.35	0.0096
0.0728	13.8	32	12.09	0.43	0.313
0.0728	28.1	32	12.09	0.43	0.527
0.0728	2.78	32	12.09	0.43	0.12
0.0728	14.03	22.2	12.08	0.40	0.375
0	13.8	22.2	12.8	0.4	0

But in current analysis, the author use existing pipe model information as stated in Nouar et al (1998) so that it is easier to make the comparison with numerical data. The fluid is full developed laminar flow and assumed to be steady state under isothermal condition. Following diagram refers a hollow cylindrical pipe model with computed mesh parameter.

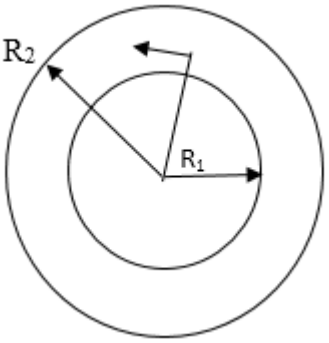

Figure 7: Annular geometry

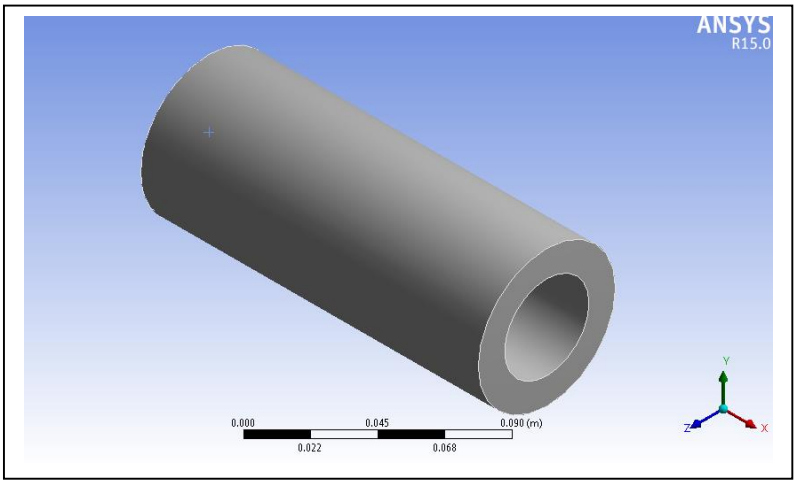

Figure 8: Concentric annular pipe

Table 5: Concentric pipe geometry

Parameter	Values	Units
Pipe inner diameter(d_i)	40	mm
Pipe outer diameter (d_o)	65	mm
Pipe length (L)	165	mm
Mesh sizing	0.002	mm
Firs aspect ratio	10	

The analysis were carried out based on inlet velocity, angular velocity, and change in Herscel Buckley model variables. Next, the results is computed in graphical form which interpret the data between benchmark and numerical analysis. The benchmark model refers to graphical analysis provided by Nouar et al (1998) based on experimental investigation data at table 3.

Next, the benchmark graph were compared with numerical analysis conduct by author using the same data from table 3. The purpose of numerical analysis here is to validate the benchmark analysis provided by Nouar et al (1998). The present work has two main motivation which is to analyse the changes in axial velocity as pipe diameter enlarge under rotational and non-rotational condition, also the effect of Hershel Bulkley fluid model on velocity profile when there is change in the model parameter that will affects the viscosity which depending on shear stress rate as related in following equations;

$$\tau = \tau_y + K_{HB}(\dot{\gamma})^{n_{HB}}$$

4.2.1 Axial Velocity profile curves

The graph in figure (a) explains the obvious differences between two data comparisons between benchmark (Nouar,1994) and numerical analysis using inlet velocity flow of u = 0.074 m/s and under no rotation condition (ω=0). The axial velocity near the pipe wall is increase until it reach the peak at 1.20 m/s and maintained until it starts decrease as the pipe diameter enlarge.

The flat axial velocity distribution obtained for the case of low Reynold number which shows not much variation in fluid flow since the flow is laminar. For the graph in figure (b), the pipe were under rotation at ω=13.8 rad/s with inlet velocity, u=0.00728 m/s.

The Reynold number is Re=0.313 which is slightly higher from the first analysis that shown in figure (a). But the flow type is still laminar. Initially, the fluid velocity is high until it reach the peak where u= 1.38m/s but decrease gradually as the pipe diameter enlarge.

There is slide variation at velocity value between figure (a) and figure (b) because the analysis in figure (b) considering pipe under rotation. The graph in figure (c) interprets that the velocity increase gradually as the pipe diameter enlarge until it reaches the peak of 1.42 m/s and decrease gradually following from the peak.

The velocity value is quite high than previous one in figure (b) because there is gradual change in pipe rotational value which affects the fluid flow velocity and overall Reynold number from Re=0.313 to Re=0.527. However, fluid still considered under laminar region.

The inner cylinder rotation induces a modification of the axial velocity profile, characterised by decrease of axial velocity gradient ($\frac{\partial u}{\partial r}$) at the outer wall of cylinder. This deformation is due to decrease of apparent viscosity inside inner cylinder where the shear rate increases due to rotation.

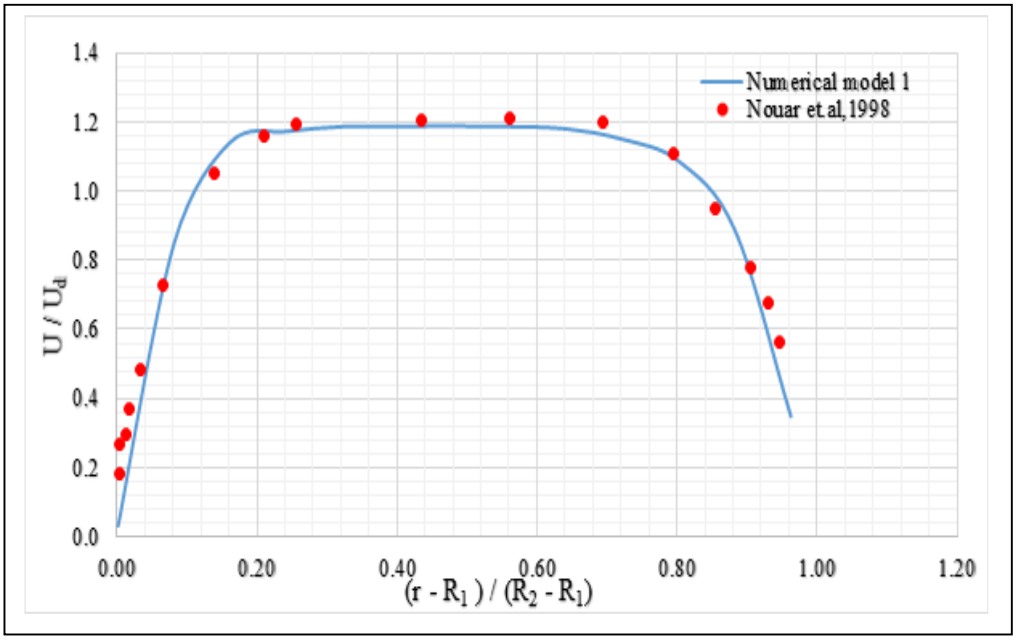

Figure 4.1 (a): Inlet velocity, U = 0.0740m/s, w (rad/s) = 0

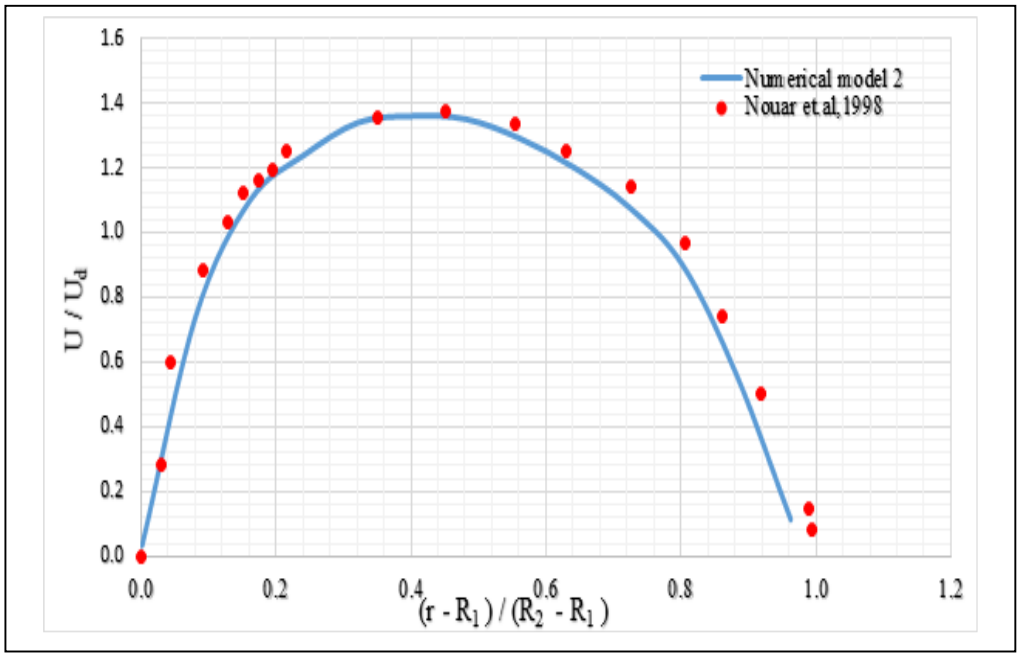

Figure 4.1 (b): Inlet velocity, u = 0.0728 m/s, ω (rad/s) = 13.8

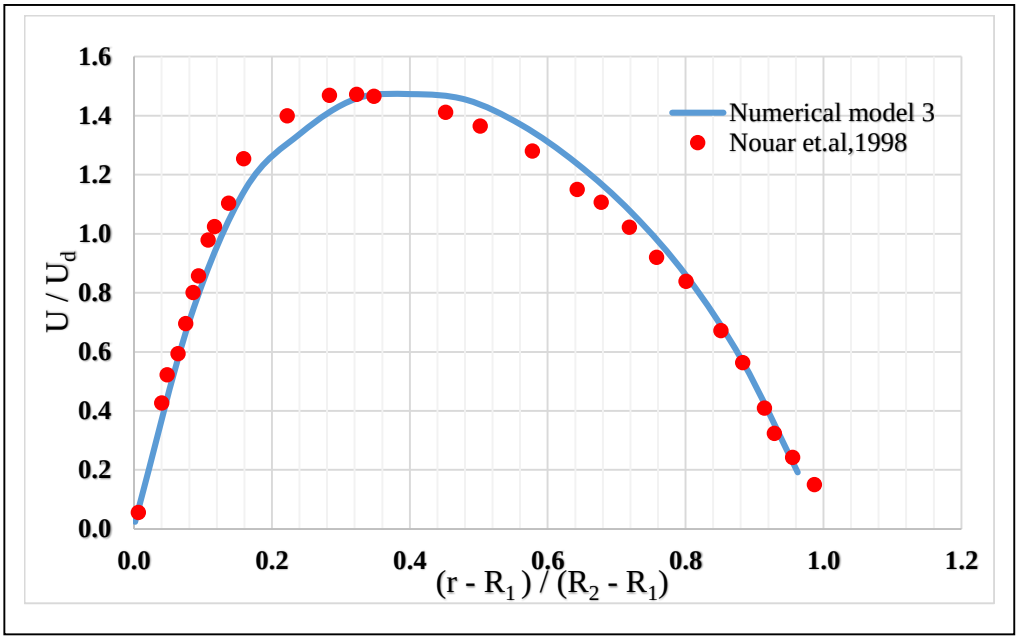

Figure 4.1 (c): Inlet velocity, u = 0.0728 m/s, ω (rad/s) = 28.1

4.2.2 Tangential Velocity Curves

The graphical analysis in figure (e) describes the tangential velocity profile that increase linearly with radial position under lower Reynold number, Re=0.12. In addition, the analysis for tangential velocity profiles make it possible to find out the effect on the rotational one. As the diameter of pipe increase, the fluid velocity gradually decrease and at one point it maintains linearity about 0.30m/s between the pipe diameter of 0.20m – 0.70m approximately at central part of pipe before it decrease pointing towards zero.

In figure (e), the velocity decreases gradually as pipe diameter increase without maintaining linearity at any point. At this point the fluid model yield stress τ_y (Pa) have slide drop from the previous model at figure (d).This could change the overall shear stress value τ that affects the fluid viscosity. When there is change in viscosity, then it either increase or decrease the Reynold number (Re) value. In these case, the Reynold number is 0.375 and it is higher from model in figure (d), Re=0.12.

In spite change in Reynold number and shear stress, the pipe rotation value also differ from previous model. Velocity profile curve in figure (e) and (f) are more similar look alike because the parameters in table 3 for the two curves are having not much different in terms of values.

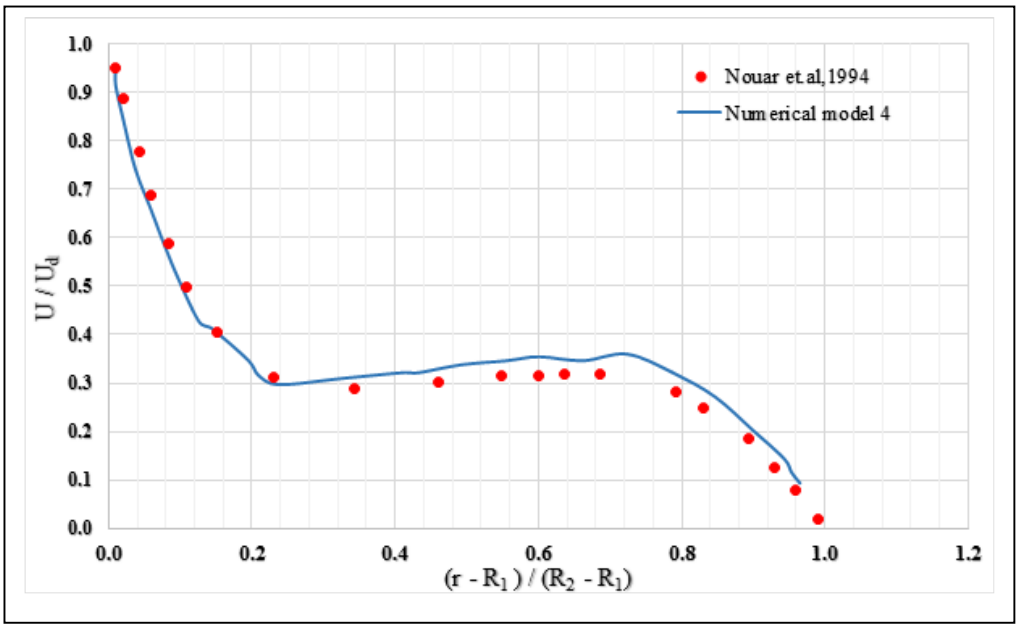

Figure 4.1 (d) Inlet velocity, u = 0.0728 m/s, ω (rad/s) = 2.78

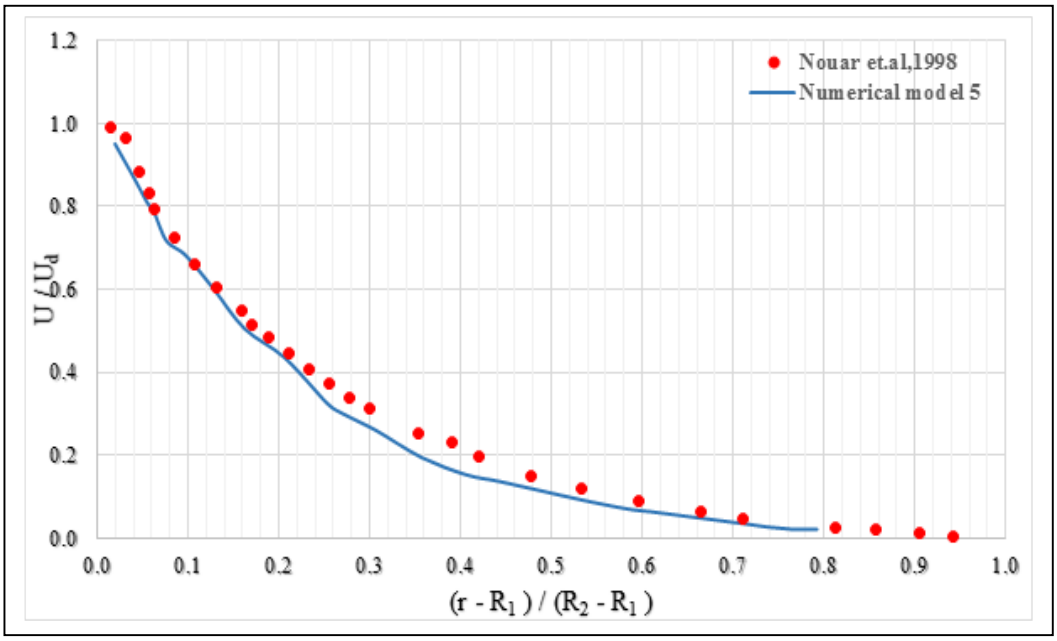

Figure 4.1 (e) inlet velocity, u = 0.0728 m/s, ω (rad/s) = 14.03

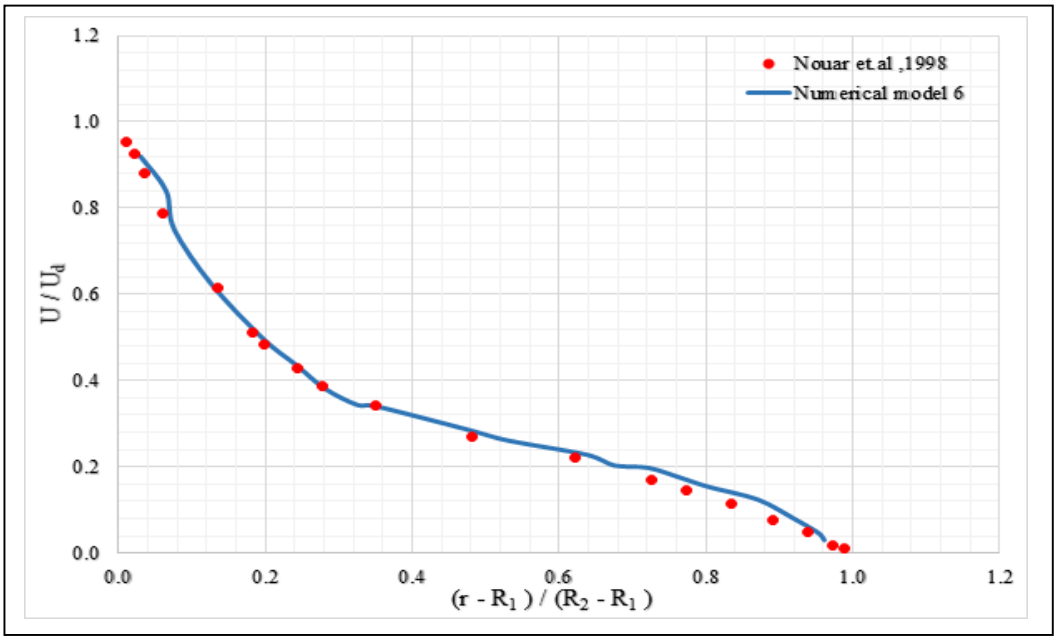

Figure 4.1 (f) Inlet velocity, u = 0 m/s, ω (rad/s) = 13.8

4.3 Case-2: Cross model (Escudier et al, 2002)

For the next case, the author would like to validate data provided by Escudier et al, 2012 in Table 6 using Cross rheological model (Cross, 1965). The drilling fluid used in following case is Carbopol 940, density $\rho =$ 940kg/m3, with concentric and eccentric annulus condition. The flow consider isothermal, fully developed flow of fluids for which the density is constant.

Table 6: Parameter data by Escudier et al (2002)

ε	U (m/s)	ω (rad/s)	μ_0	μ_∞	K_{CR}	n_{CR}	Re	Ta
0	0.203	5.24	0.159	0.00273	1.305	0.509	236	6020
	0.202	3.14	0.142	0.00240	0.963	0.515	228	2026
0.8	0.268	5.35	0.177	0.00255	0.630	0.551	225	3172
	0.268	5.24	0.262	0.00144	2.414	0.504	241	3500

Following data from Escudier et al (2002) describes the dimensions in term of radius of pipe geometry for sector A, B, C and D under concentric and eccentric annulus condition with rotation. From the data in table 5, the velocity profile against pipe diameter were plotted which indicates the velocity flow behaviour at pipe wall and centre during rotation.

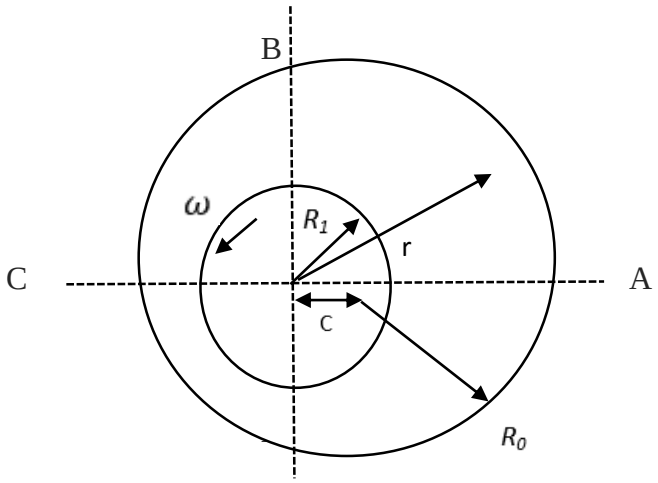

Figure 9: Annulus cross sectional pipe geometry

Using the following data, axial and tangential velocity profile graphs have been plotted. The axial velocity profile is known as change of velocity across change in pipe radius ($\frac{\partial u}{\partial r}$) at the wall of outer cylinder. This change is due to change in viscosity that increase shear rate due to rotation. The tangential velocity profile increase linearly with radial position.

Table 7: Pipe radius dimensions for Sector A, B, C&D

ε	**Min radius (r, mm)**	r_1 **(A) (mm)**	r_2 **(B) (mm)**	r_3 **(c) (mm)**	r_4 **(D) (mm)**	**U (m/s)**	ω **(rad/s)**
0	25.4	70.04	46.11	30.36	46.11	0.268	5.24
	25.4	70.04	46.11	30.36	46.11	0.268	3.14
0.8	25.4	70.04	46.11	30.36	46.11	0.268	5.35
	25.4	70.04	46.11	30.36	46.11	0.268	5.24

Following is the equations for Cross model (Cross, 1965)

$$\frac{\mu_0 - \mu_\infty}{\mu - \mu_\infty} = 1 + K_{CR}\dot{\gamma}n_{cr}$$

Or;

$$\mu = \mu_\infty + \frac{\mu_0 - \mu_\infty}{1 + K_{CR}\dot{\gamma}n_{cr}}$$

The values for the consistency index K_{CR} and the exponent n_{cr} are listed in table 6. Few conditions were considered such as isothermal, laminar flow regime, fully developed in such ways the density of the fluid will be constant and the viscosity dependent on shear rate, $\dot{\gamma}$. The Reynold number for the case study expressed in by following equation (Escudier et al, 2002):

$$Re = \frac{2\rho U\delta}{\mu_F}$$

Taylor number;

$$Ta \equiv \left[\frac{\rho\omega}{\mu_F}\right]^2 R_I\delta^3$$

The viscosity μ_F that dependent on characteristic of shear rate for the flow, (γ_F) defined by as following;

$$\gamma_F = \frac{\dot{\gamma}_F \delta}{U} = \frac{1}{2}\sqrt{(1+\xi^2}$$

Initially, Cross model equation were not found under CFX analysis. However, an additional expressions of Cross model variables were added to run the simulations which considered as numeral analysis and finally compared with benchmark analysis by Escudier et al, (2002). To compromised the difference between numerical and Escudier et al (2002) benchmark analysis, few changes has been taking into account as following;

$U = \frac{\mathrm{u}}{\mathrm{U_d}}$; u: axial velocity from graph, $\mathrm{U_d}$: Bulk mean velocity

$(\mathrm{r} - \mathrm{R_1}) / (\mathrm{R_2} - \mathrm{R_1})$; r: axial pipe radius values from graph

4.3.1 Axial velocity profiles at, $\epsilon = 0.8$

Figure below shows comparison between numerical and benchmark analysis (Escudier et.al, 2002) from the experimental investigation data provided by Escudier et al (2002) under eccentricity condition, $\epsilon = 0.8$

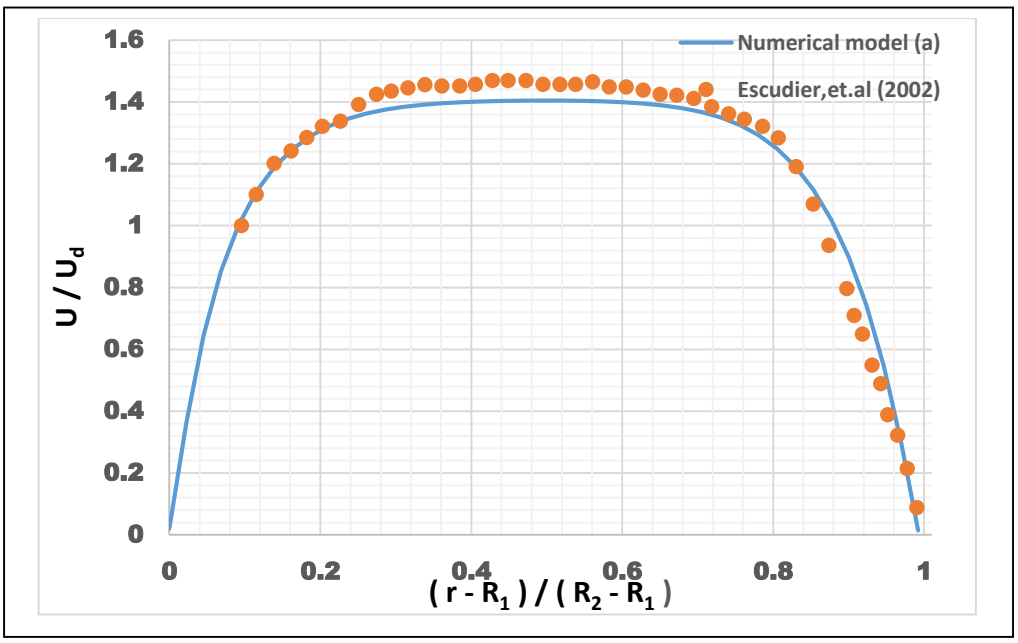

Figure 4.2 (a) Ta: 3500, Re: 241, U: 0.268 m/s, ω: 5.24 rad/s

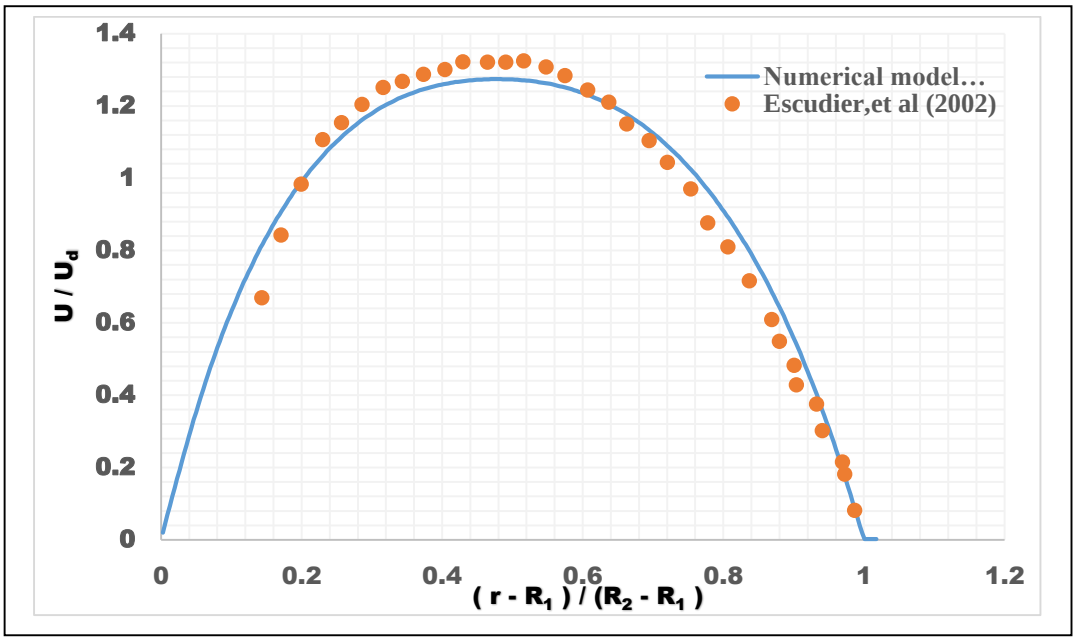

Figure 4.2 (b) Ta: 3500, Re: 241, U: 0.268 m/s, ω: 5.24 rad/s

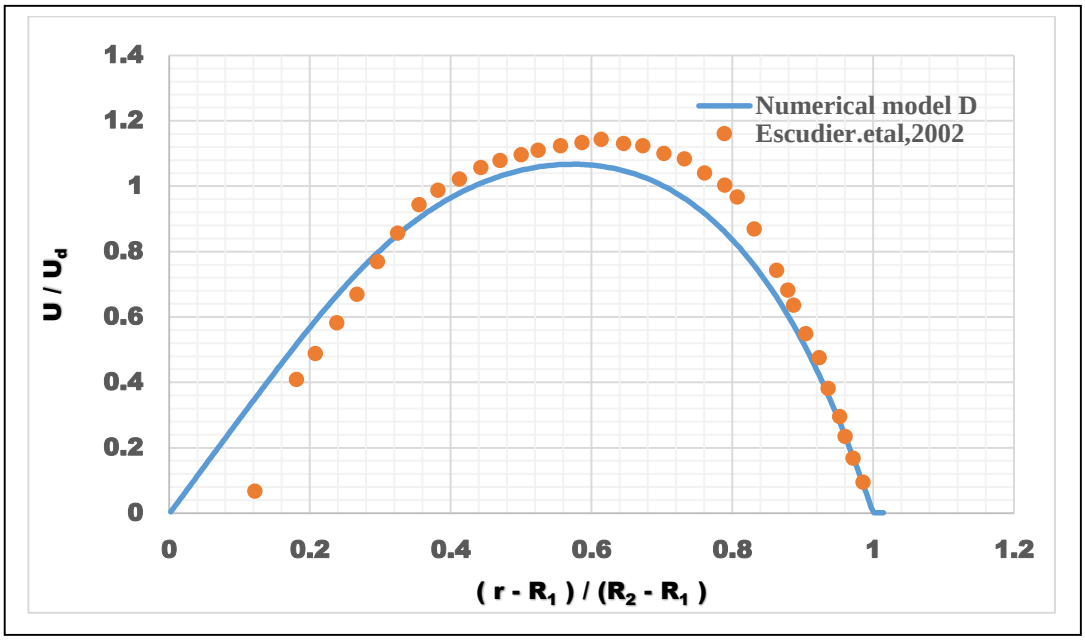

Figure 4.2 (c) Ta: 3500, Re: 241, U: 0.268 m/s, ω: 5.24 rad/s

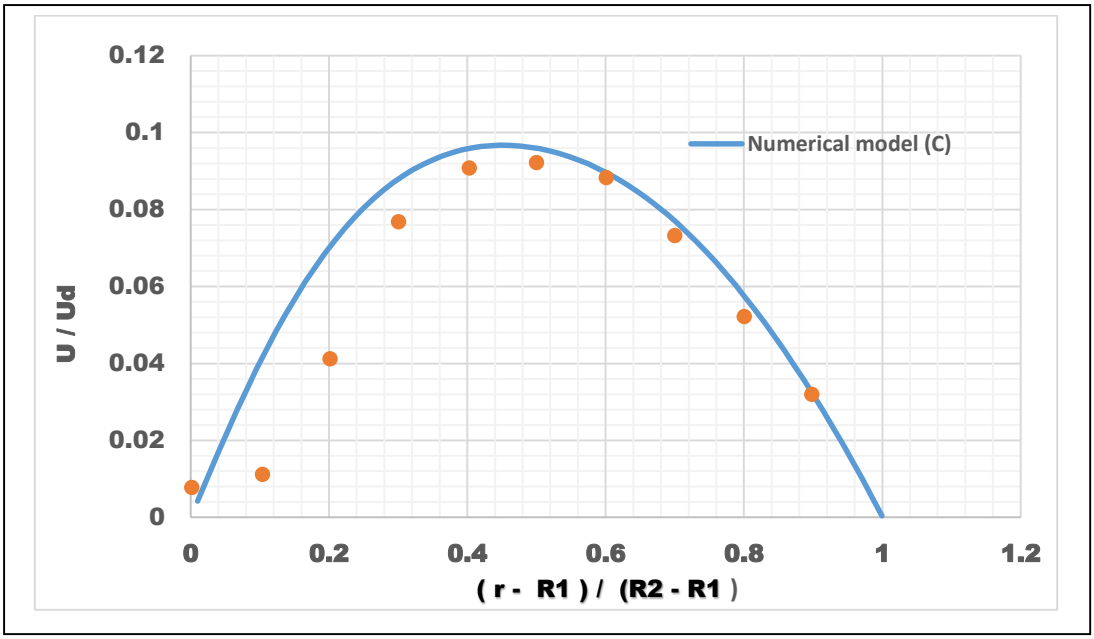

Figure 4.2 (d) Ta: 3500, Re: 241, U: 0.268 m/s, ω: 5.24 rad/s

4.3.2 Tangential velocity profiles at, $\epsilon = 0.8$

Figure below shows comparison between numerical and benchmark analysis Escudier et.al, (2002) from the experimental investigation data provided by Escudier et al (2002) under eccentricity, $\epsilon = 0.8$ condition for tangential velocity data.

Sector A, B, C& D shows the axial velocity profile curves against pipe diameter. From the simulation results obtained, there are difference between numerical and benchmark analysis produced by Escudier et al, (2002). The general level agreement is same for pipe geometry, Cross model variable expressions and fluid model characteristic. But the meshing is one constraint to get similar velocity profile.

For axial and tangential velocity profile curves, the calculations have capture all the necessary features revealed by the data. The greatest difference with tangential velocities are at area near inner cylinder at wide gap (A) and the narrow gap (C). While for axial velocity, is the widening gap possibly due to offset between two different cylinders that varies with different radial dimension.

Otherwise, the axial velocity profile interprets that the velocity profile increase along near pipe wall as the pipe radius increase. But the velocity profile maintains at pipe centre but decrease gradually as the radius keep increasing. The expressed axial velocity profile curves is for Re = 225, Ta = 3172. For tangential velocity profile curve, there is slight increase in Reynold number, Re = 241 with Ta = 3500. The curve focus on velocity profile along the radial position which it approaches to zero as the pipe radial dimension were increase gradually.

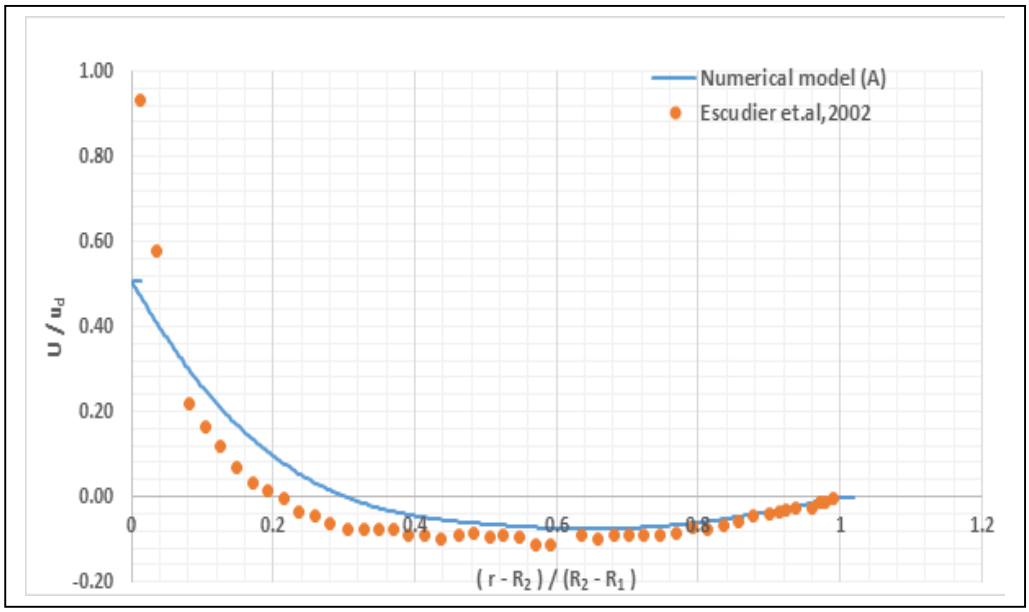

Figure 4.2 (e), Re: 241, U: 0.268 m/s, ω: 5.35 rad/s

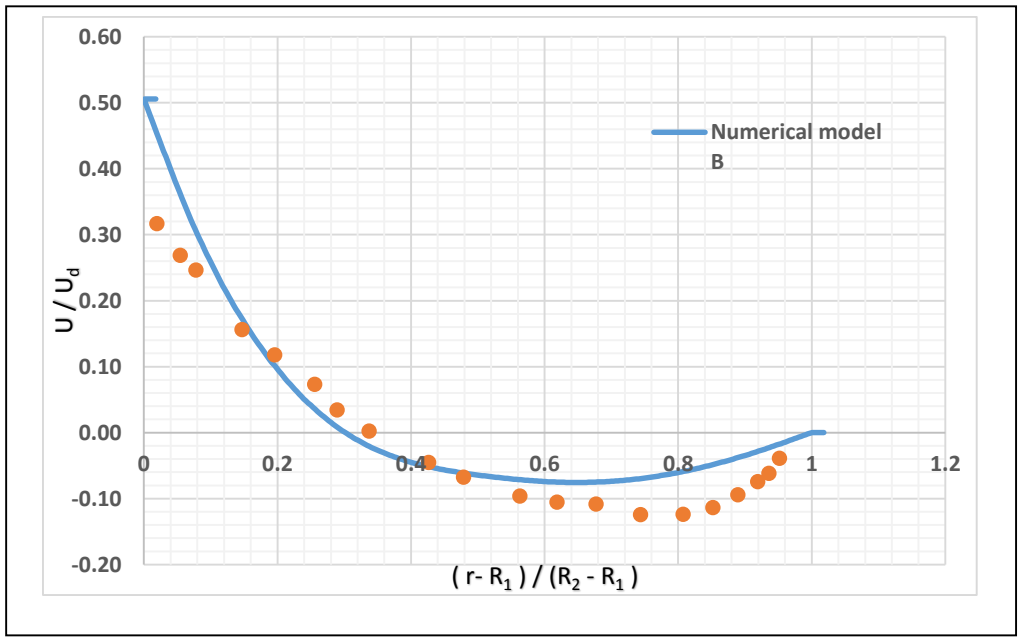

Figure 4.2 (f) Ta: 3172, Re: 241, U: 0.268 m/s, ω: 5.35 rad/

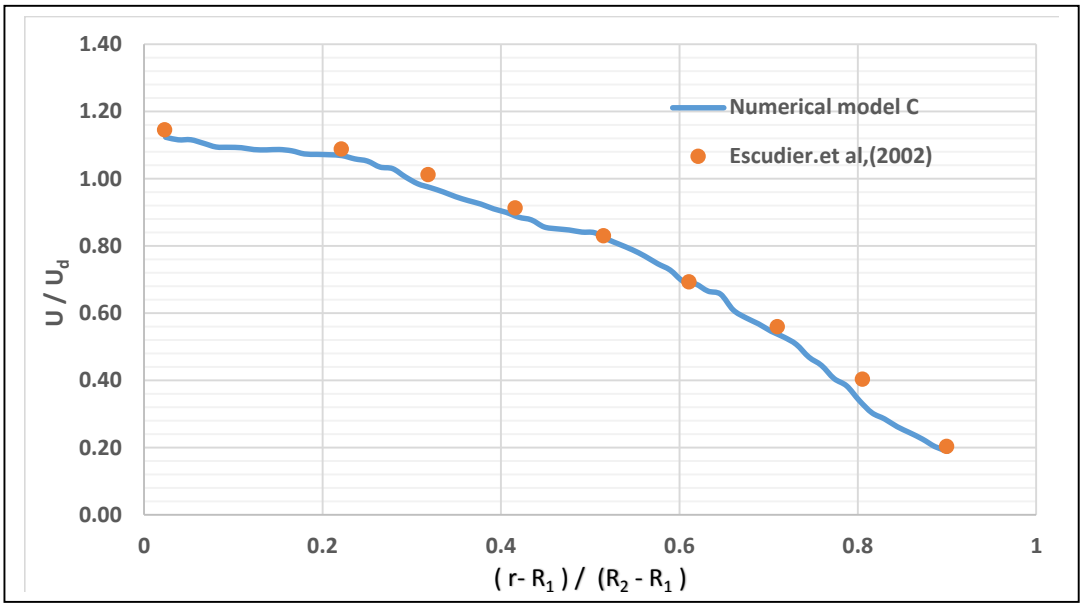

Figure 4.2 (g) Ta: 3172, Re: 241, U: 0.268 m/s, ω: 5.35 rad

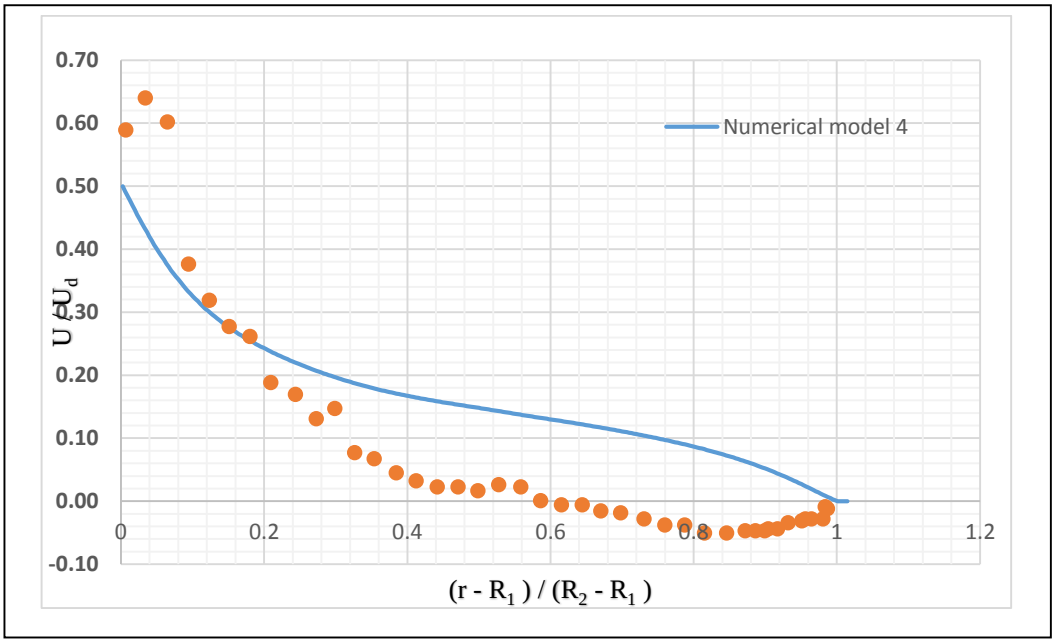

Figure 4.2 (h) Ta: 3172, Re: 241, U: 0.268 m/s, ω: 5.35 rad/S

4.4 Pressure gradient using Design on Experiment (DOE) method

The pressure gradient is determine by using three variables which are inlet velocity (V_{in}), pipe rotation (ω) and eccentricity (ε). Thus, an upper and lower limit values is been set to identify the pressure gradient between the stated variables at designated analysis range that shown in table below;

Table 8: Parametric values of DOE

Parameter	**Lower limit**	**Average**	**Upper limit**
Inlet velocity, ($V_{in,}$ m/s)	0.1	1.6	3.1
Pipe rotation, (ω, rad/s)	1.5	10.15	20
Eccentricity,(ε)	0.1	0.5	0.95

The above sets of data will be used to generate Design of Experiment (DOE) points using ANSYS under CFX analysis. The purpose of generating the data is to calculate the pressure difference with linear increase of pipe diameter using above parameter variables that have been grouped between upper and lower limit values. Latin Hypercube is the sampling method that have been selected to generate the points.

Another sampling technique is known as Central Composite Design (CCD) but it is not suitable for large design sets of variables and will be time consuming to get an outcome. The analysis only focus on centre points and unlike Latin Hypercube that consider that ensures every variable is represented and no matter the response is dominated by few number of points. Another advantage is the number of points can be directly defined.

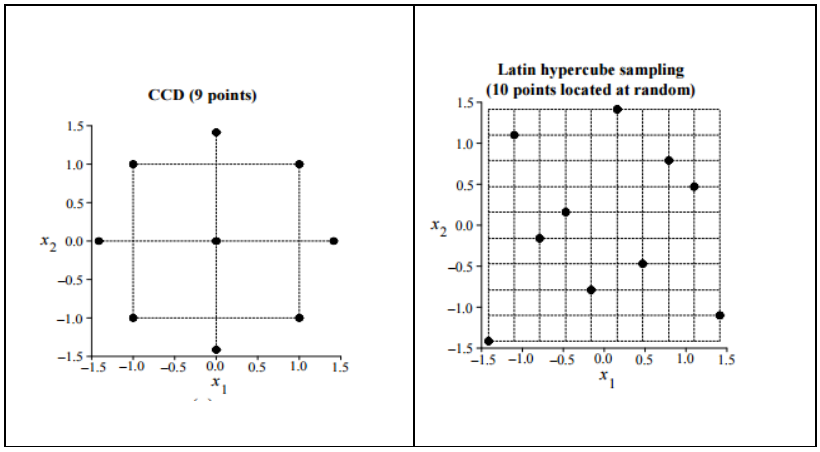

Figure 7: Difference between CCD and Latin Hypercube sampling

Following table refers to Design of Experiment (DOE) points generated using Latin Hypercube sampling techniques with pressure gradient analysis;

Table 9 Design of Experiment (DOE) points

Name	vin (m/s)	w (rad/s)	e(1)	Offset (mm)	Dp/dx (kg/m2.s2)
1	1.8	15.6833	0.582	14.425	1405.334
2	2.4	10.75	0.638	15.381	1824.05
3	0.2	11.98333	0.242	5.993	110.344
4	2.2	2.116667	0.865	21.452	1480.914
5	0.4	4.583333	0.298	7.399	242.931
6	3	3.35	0.185	4.588	3700.236
7	2	18.15	0.808	20.047	1284.881
8	2.8	14.45	0.752	18.641	2456.978
9	1	5.816667	0.525	13.02	490.614
10	0.8	13.21667	0.922	22.857	454.971
11	1.4	8.283333	0.412	10.209	784.301
12	0.6	16.91667	0.355	8.804	309.89
13	1.6	9.516667	0.468	11.615	1667.525
14	2.6	19.8333	0.128	3.183	3409.5
15	1.2	7.05	0.7	17.24	645.406

The above pressure gradient values is knows as response points. Response point is a snap shot parameter values where the output parameter values were calculated from variables in Design of Experiment (DOE) data from a response surface. Using the generated the response points, the following charts have been plotted;

Figure 8 (a) shows the response curve relations between pressure gradient and velocity. The graph shows that pressure gradient proportionally increase with inlet velocity or typically known as axial velocity flow. The pressure gradient here is driving force to push the fluid to flow through a pipe.

In other words, when the flow rate is increase by axial velocity, the pressure gradient will be high and tendency the fluid to push is more across the pipe length. This condition applied for laminar regime under fully developed condition.

Figure 8 (b) shows the 3 Dimension response chart plot that indicates the peak, average and normal plot according colour variation. In figure 8 (c), shows the response curve for pressure gradient and eccentricity. The graph explains the pressure gradient decrease when the pipe eccentricity increases.

Eccentricity here known as offset values between two cylindrical pipes from the origin. Figure 8 (d) shows the 3 Dimension (3D) response chart for Pressure gradient and Eccentricity with different colour variation that indicates its peak, average and normal eccentricity and pressure gradient values.

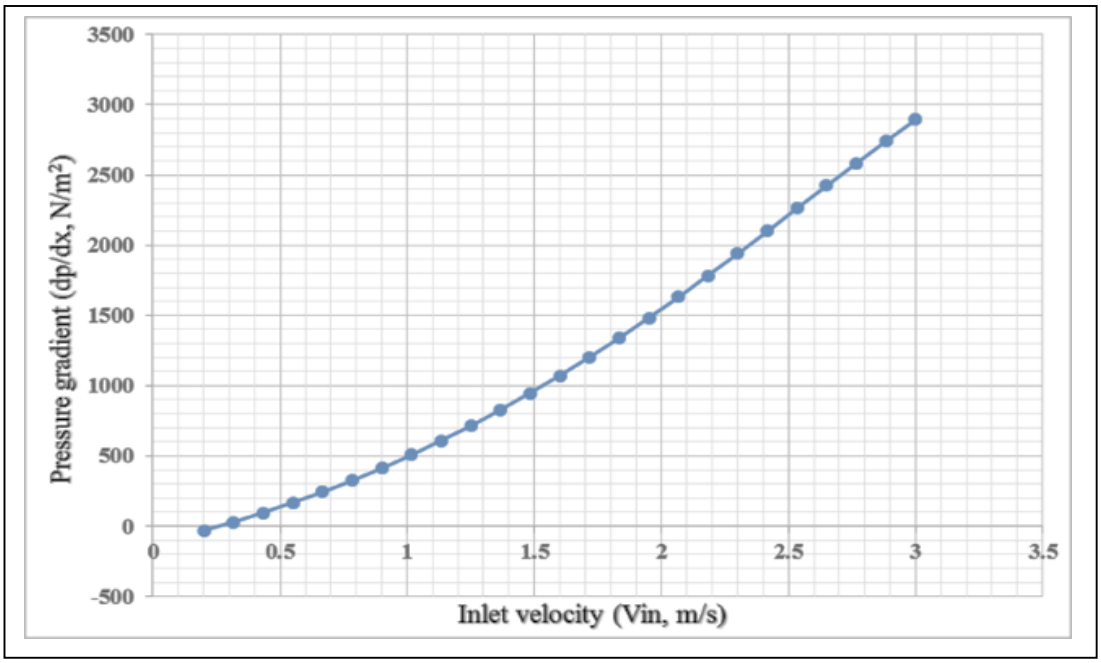
Pressure gradient (dp/dx, N/m²)
Inlet velocity (Vin, m/s)
3500
3000
2500
2000
1500
1000
500
0
-500
0
0.5
1
1.5
2
2.5
3
3.5

(a)

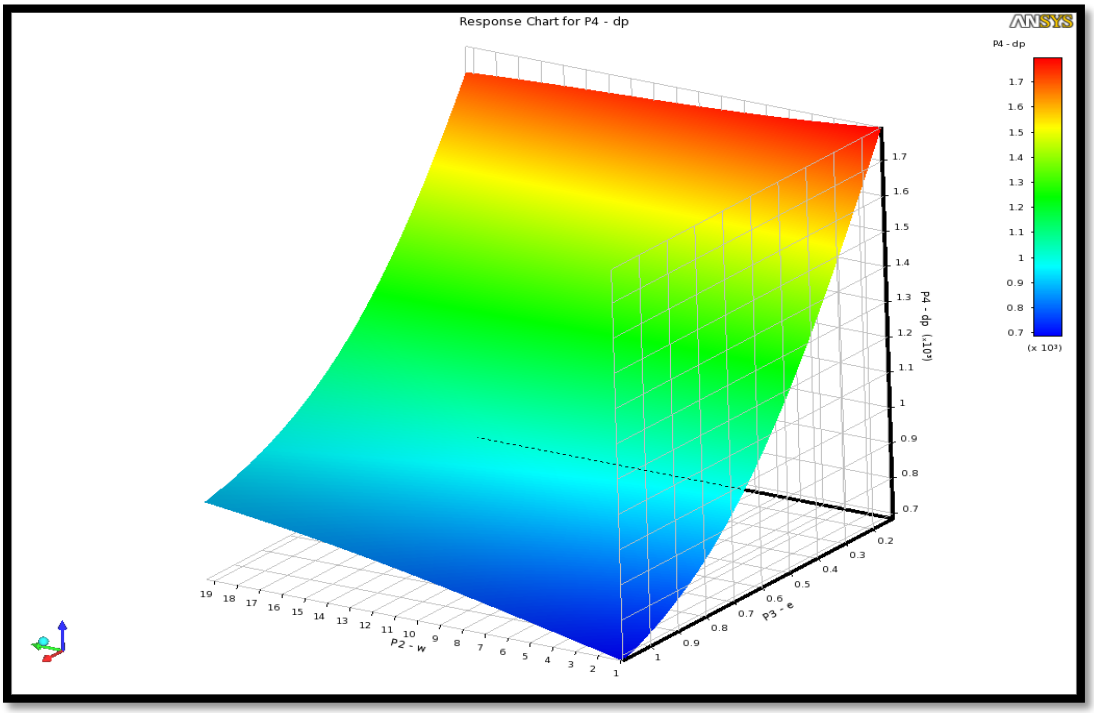
Response Chart for P4 - dp
ANSYS
P4 - dp
P4 - dp (x10³)
(x 10³)
P2 - w
P3 - e

(b)

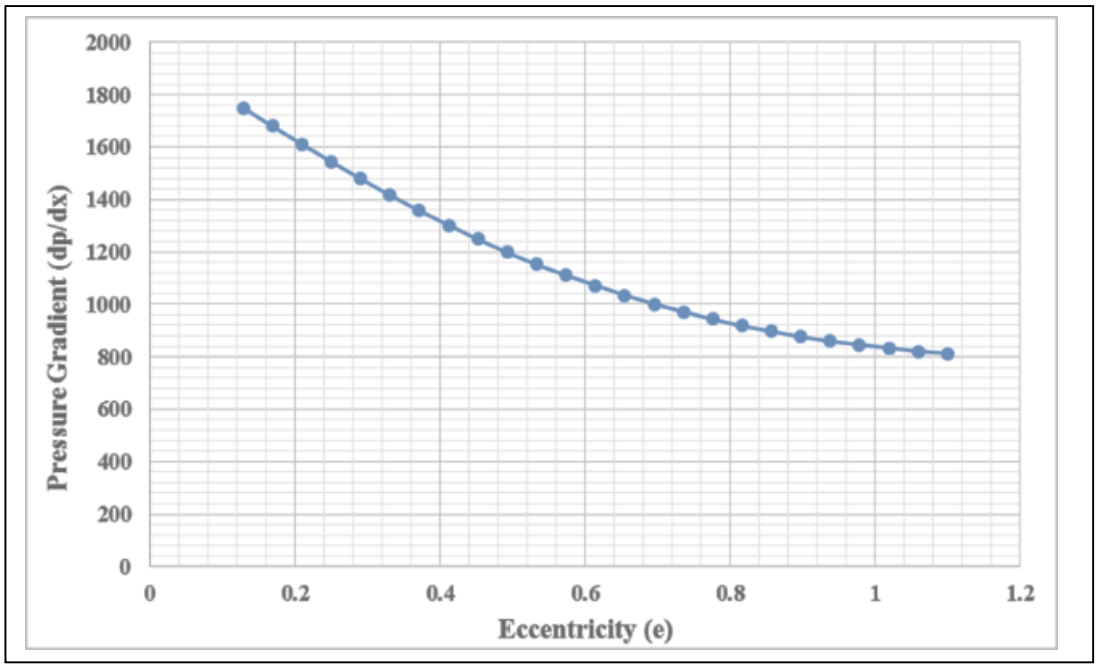

(c)

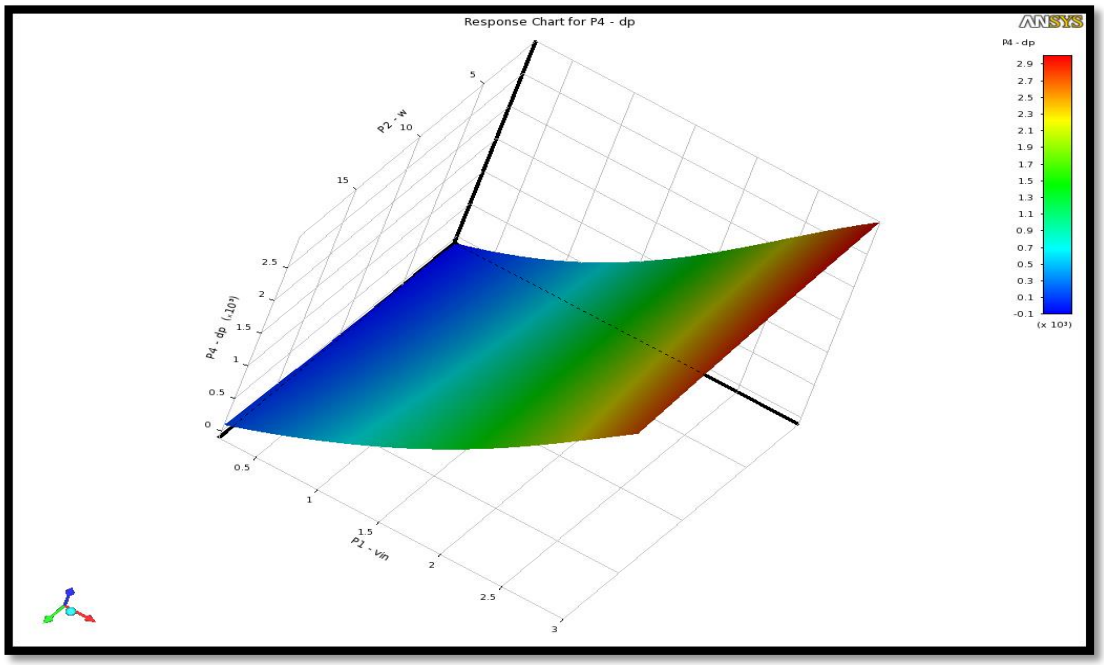

(d)

Figure 9: Plot for pressure gradient: (a) dp/dx vs inlet velocity, (b) velocity step response, (c) dp/dx vs eccentricity, (d) eccentricity step response

4.5 Oil Based Mud (OBM) flow behaviour using Sisko's model

The design points above were generated using Latin Hypercube sampling. Following is the 2D and 3D response curves for pressure gradient against eccentricity, inlet velocity, inclination and rotation. At first place, the pressure drop decrease with increasing velocity as shown in figure 4.5(a) but increase linearly beyond certain point which validated in figure 4.4 (a).

But the situation is different for cases involving inlet eccentricity and rotation due to taking into account on inclination factor. The pressure gradient graph is plotted by running the simulation for 25 number models as shown in Table 4 in appendices.

For an each individual model, the drill pipe is modelled using a hydraulic length in Table 5 in appendices and then use meshing to simulate the results. The pressure loss is determine using gradient difference method and then export back to DOE to determine generate the response curve and shown in following figures.

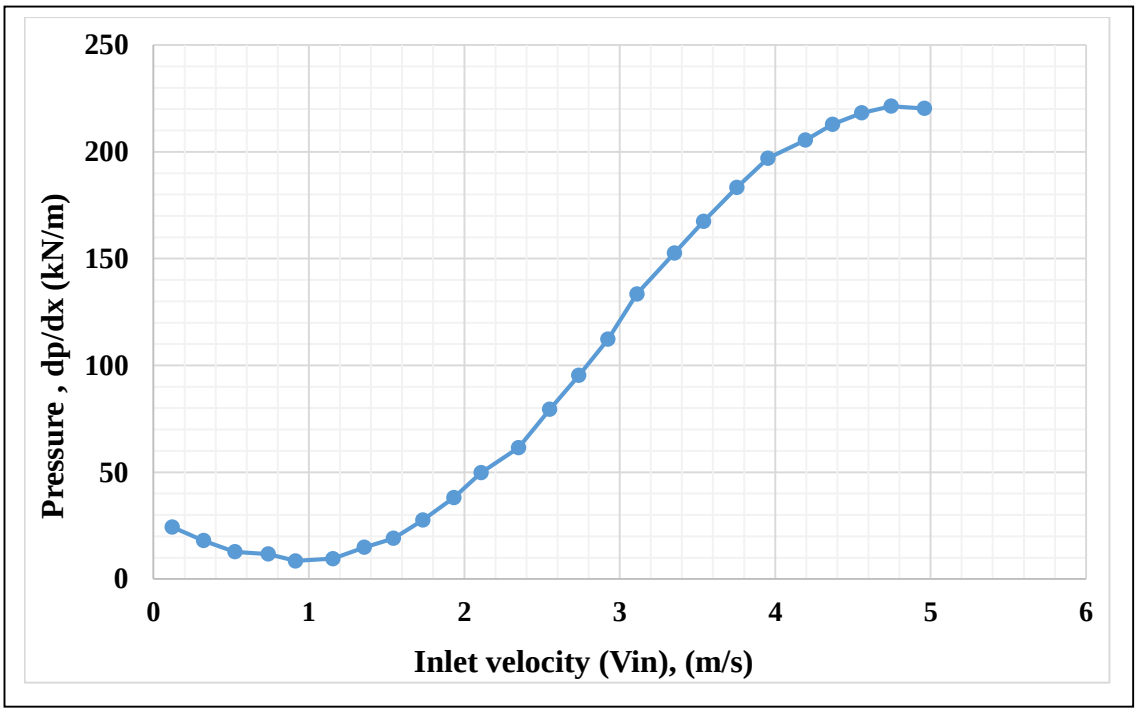

(a)

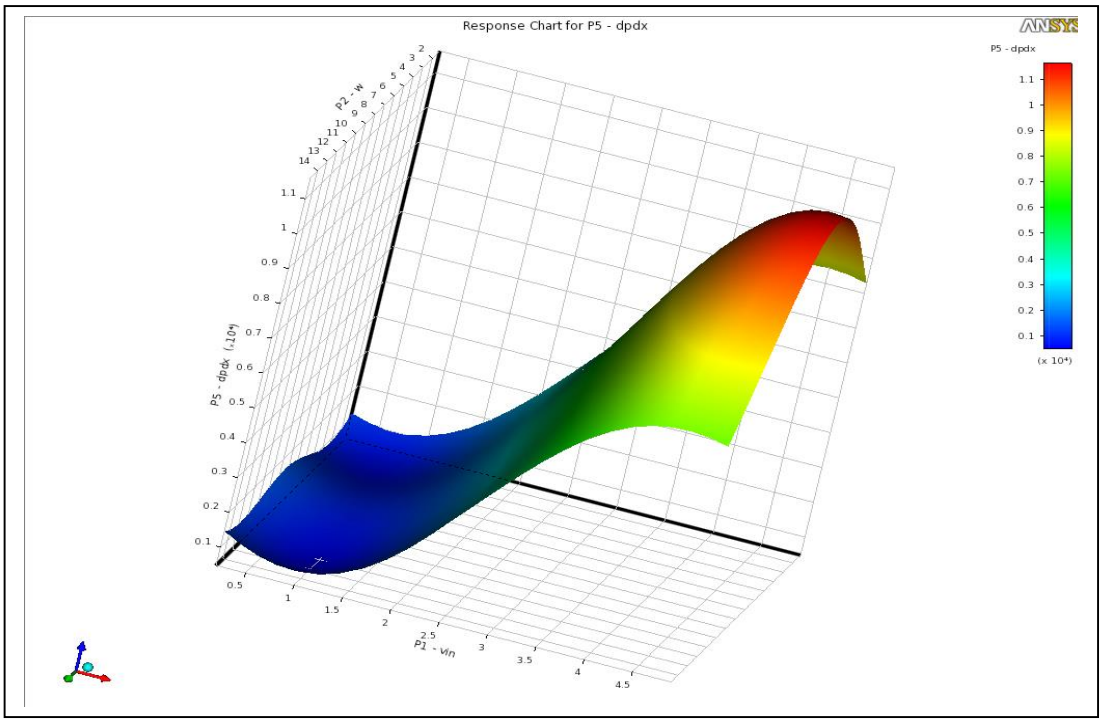
Response Chart for P5 - dpdx
P5 - dpdx
P2 - w
P5 - dpdx (x10^4)
P1 - vin

(b)

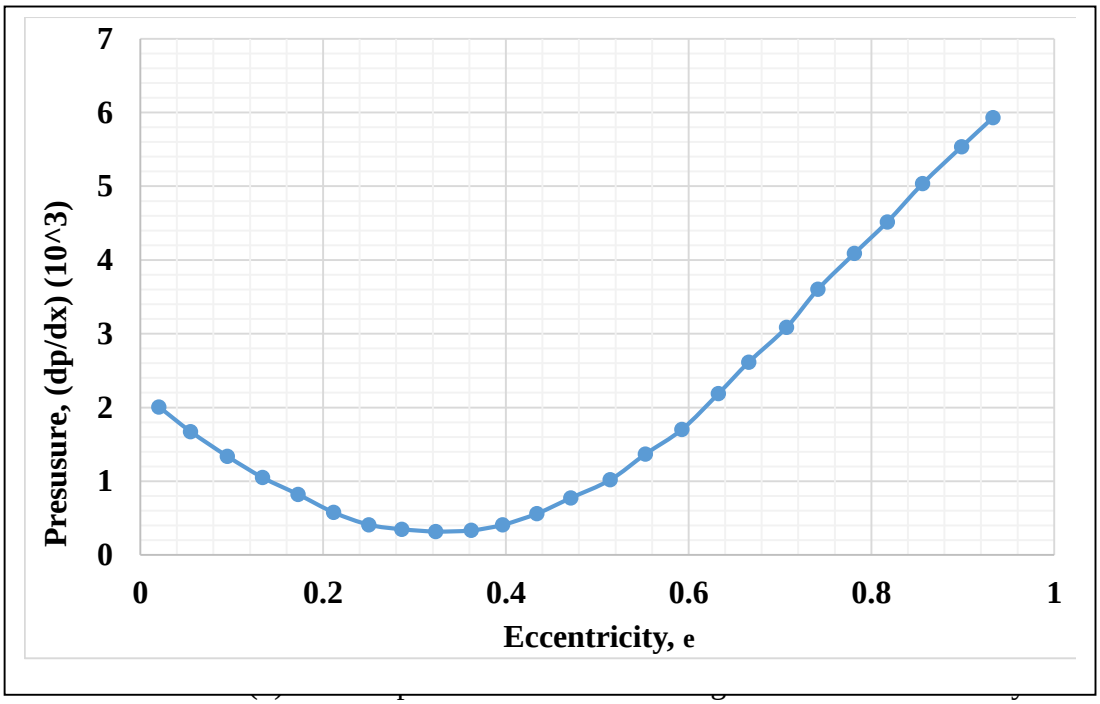
Presusure, (dp/dx) (10^3)
Eccentricity, e
0
1
2
3
4
5
6
7
0
0.2
0.4
0.6
0.8
1

(c)

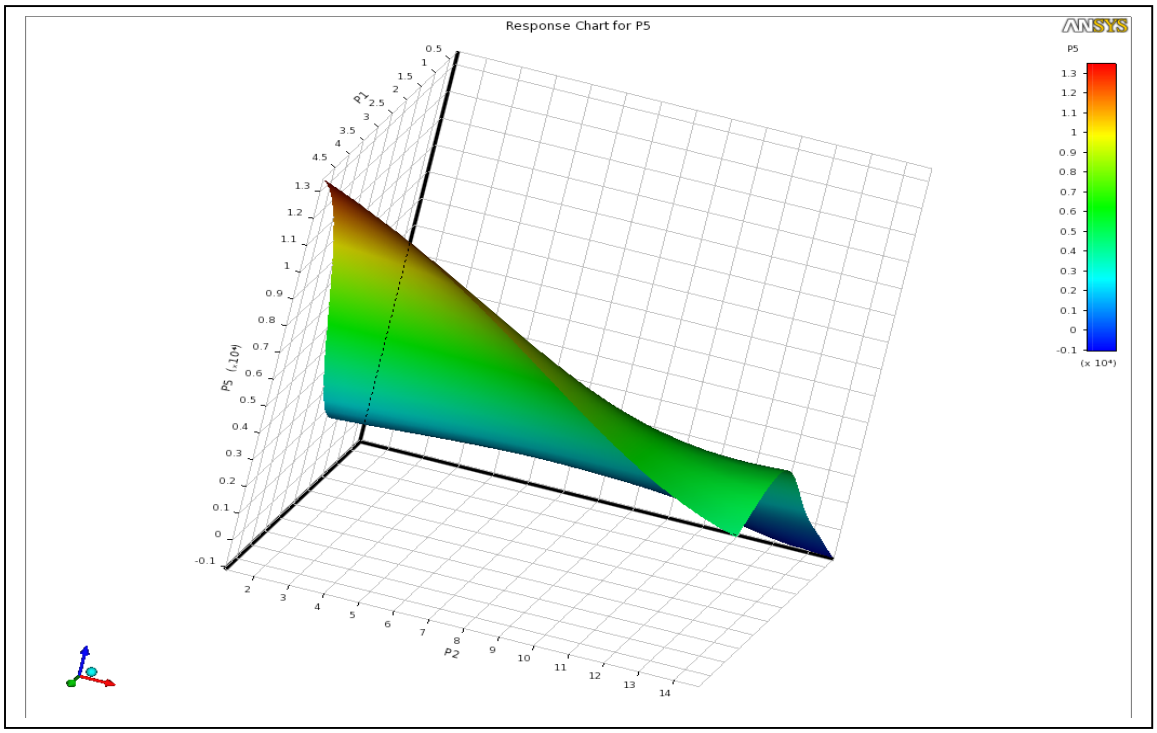
Response Chart for P5
ANSYS
P5
(x 10⁴)
P1
P2
P5 (x10⁴)

(d)

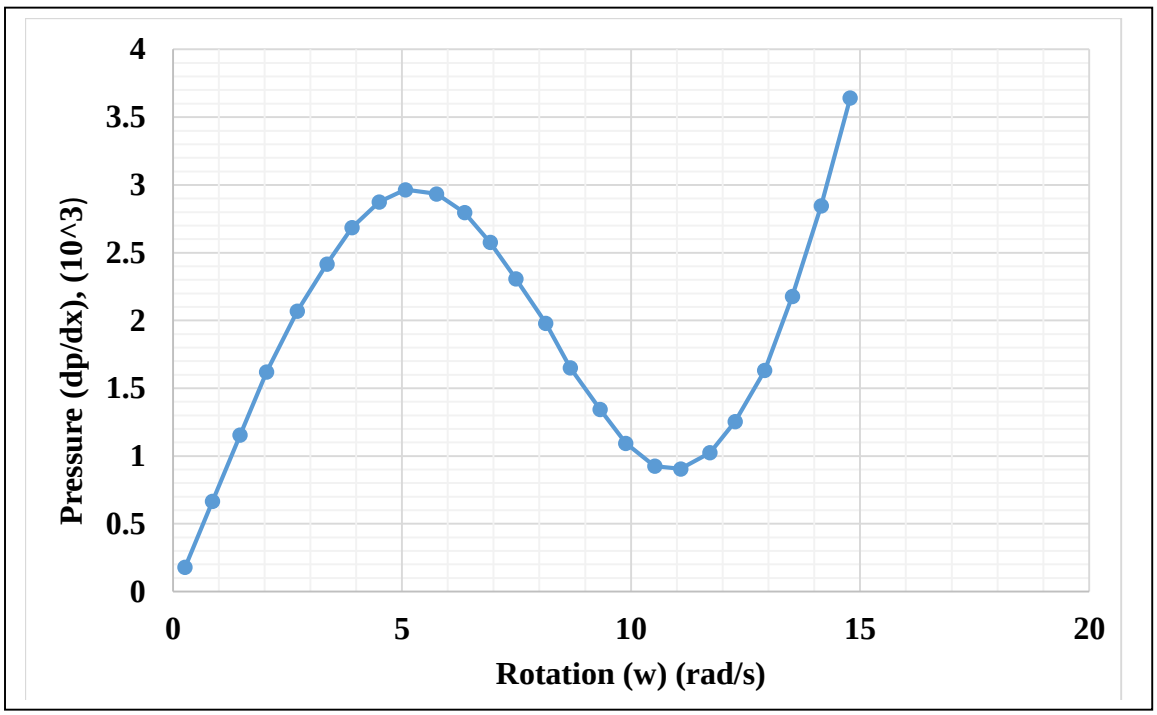
Pressure (dp/dx), (10^3)
Rotation (w) (rad/s)
0
0.5
1
1.5
2
2.5
3
3.5
4
0
5
10
15
20

(e)

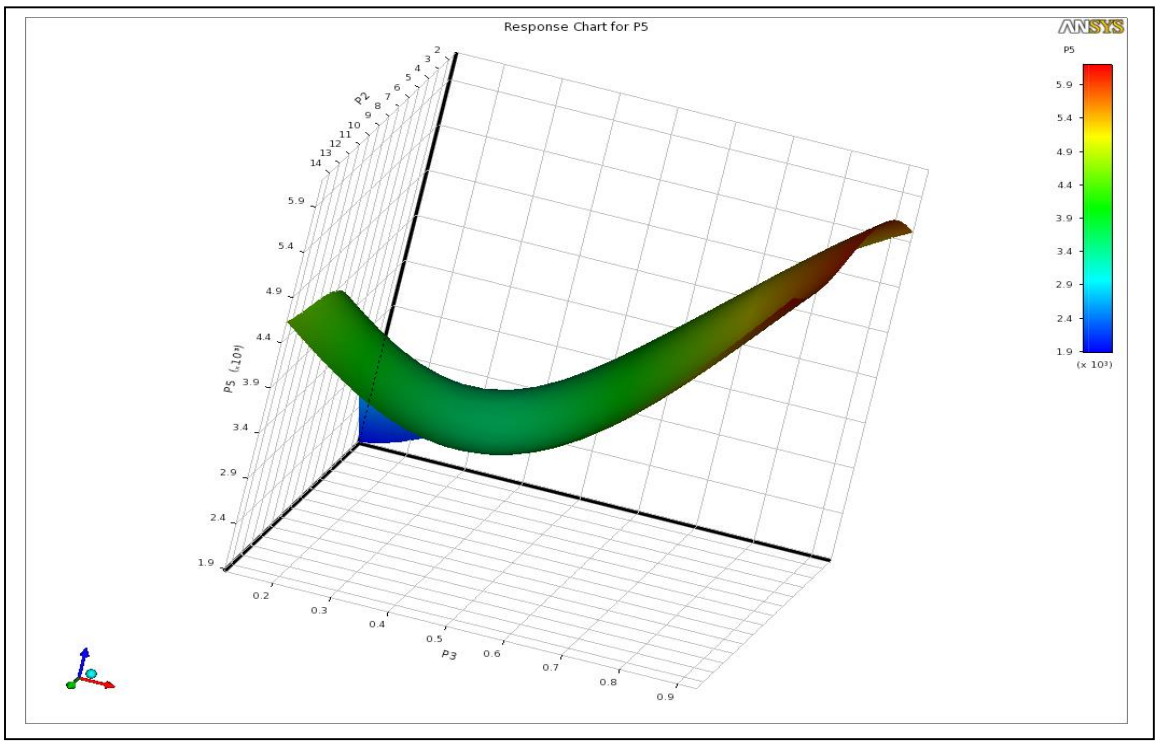
Response Chart for P5
ANSYS
P5
5.9
5.4
4.9
4.4
3.9
3.4
2.9
2.4
1.9
(x 10³)
P2
P5 (x10⁹)
P3
0.2
0.3
0.4
0.5
0.6
0.7
0.8
0.9

(f)

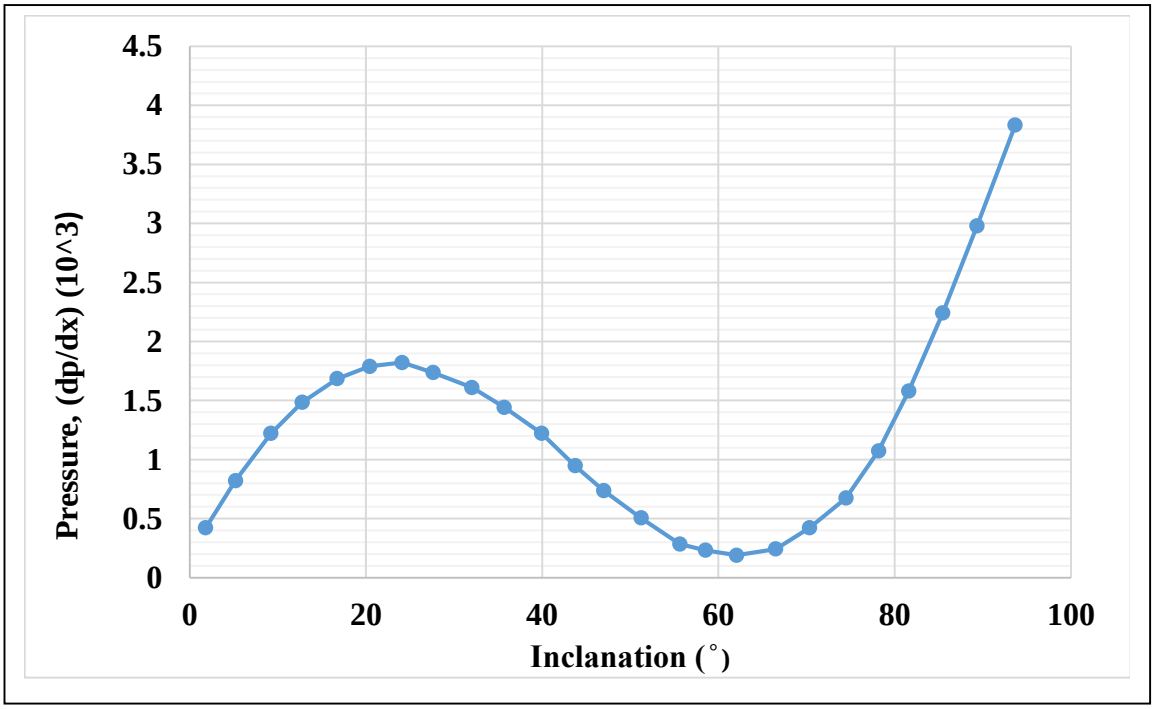
Pressure, (dp/dx) (10^3)
4.5
4
3.5
3
2.5
2
1.5
1
0.5
0
0
20
40
60
80
100
Inclanation (˚)

(g)

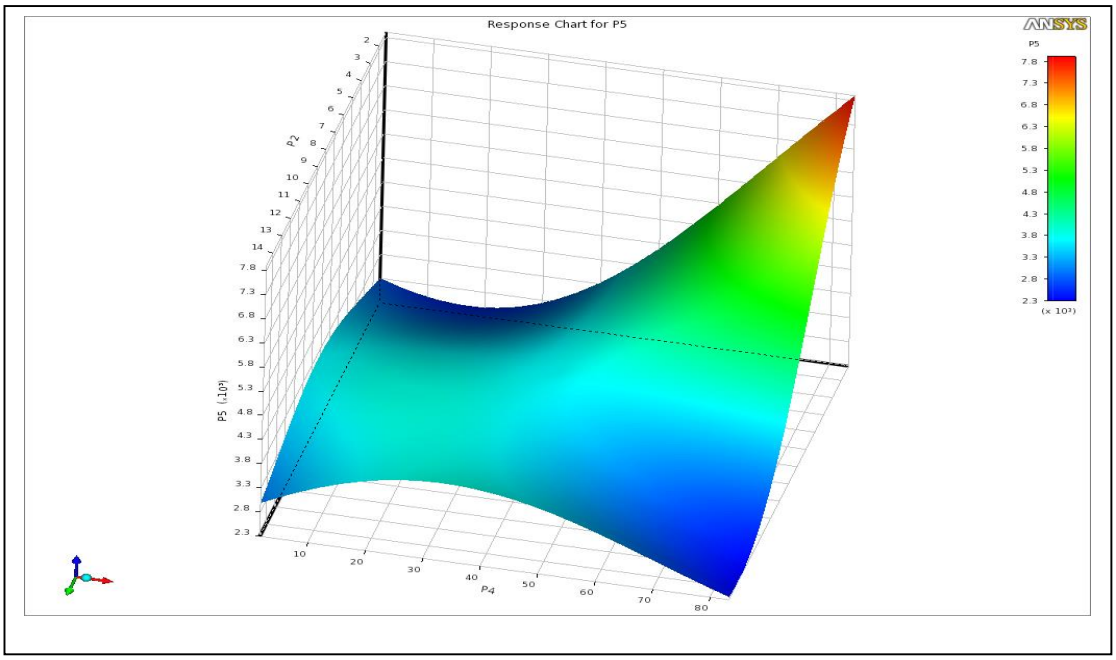

(h)

Figure 10: Plot for pressure gradient: (a) dp/dx vs inlet velocity, (b) velocity step response, (c) dp/dx vs eccentricity, (d) eccentricity step response, (e) dp/dx vs rotation, (f) rotation step response, (g) dp/dx vs inclination, (h)) inclination step response.

CHAPTER 5: CONCLUSION AND RECOMMENDATION

5.1 Conclusion

The investigation of effects of drillstring dynamics in mud flow behavior for concentric pipe by selecting benchmark cases from Nouar et al. (1998) and Escudier et al. (2002) have been validated using Carbopol 940 (non-Newtonian) as drilling fluid before proceed with an actual case using Oil Base Mud (OBM). The rheological model determines the behaviour of fluid flow in concentric pipe and the rheological model for benchmark cases are Herschel Buckley and Cross model.

The next phase of the research is **to** explore the pressure loss relationship among inlet velocity, eccentricity and rotational effect along inclination under an eccentric pipe. The drilling fluid used here was Oil Based Mud (OBM). To be precise it is B128 Bentonite. Oil based Mud (OBM) have good lubrication and boiling points properties and stable at high temperature. But this research only consider the flow behaviour under laminar flow regime at isothermal condition.

Sisko's model have been used to determine the viscosity selection. Initially, The DOE method is been used to generate the points involving inlet velocity, eccentricity, rotation, and theta using upper and lower boundary limits with Latin hypercube sampling solver. The results from the analysis have been discussed briefly in results and discussion session. Later, it were exported back to no meshing to solve the pressure gradient along the manipulated variables using Reynold number and taylors number as a solver.

5.2 Recommendation

It is recommended for the future research to study on interfacial forces which includes parameters such as lift, drag and considering kinetics granular theorem to investigate pressure drop relationship on mud flow behavior by varying the drill pipe angle, velocity, angular velocity (rotations) at different inclination using Sisko's model. Furthermore, the suggestion for scope includes multiphase flow study on cutting transport efficiency towards mud flow behavior.

REFERENCES

Bilgesu HI, Ali MW et al. (2002) Computational fluid dynamics (CFD) as a tool to study cutting transport. In: SPE Eastern

Escudier.M.P,Olievera.P.J,Pinho.F.T,Smith.S, (2002) Fully developed laminar flow of non-Newtonian liquids through annuli; comparison of numerical calculation with experiments, Experiment in fluids 33 (2002) 101-111

Ekambara.K,SeanSandres.R,Nandakumar.K,Masliyah.J.H,(2009) Hydrodynamic Simulation of Horizontal Slurry Pipeline Flow using ANSYS-CFX, University of Alberta, Canada,48: 8159-8171

Hermoso.J,Martinez.B.F,Gallegos.C (2014) Influence of Viscosity modifier nature and concentration on the viscous flow behaviour of oil based drilling fluids at high pressure, Applied Clay Science 87(2014),14-21

Iyoho, A. W., Azar, J. J.: "An Accurate Slot Model for Non-Newtonian Fluid Flow through Eccentric Annuli", SPE J. (Oct. 1981), pp. 565-572.

Luo, Y. and Peden, J. M. "Flow of Drilling Fluids through Eccentric Annuli",

Khodja,M.,Canselier,J.P,.Bergaya,F.,Fourar,K.,Khodj,M.,Cohaut,N., Shale problems and water based drilling fluid optimization in the Hassi Messaoud Algerian oil field, Appl ClaySci.49, 383-393

Nouar C, Desaubry C,Zenaidi H (1998) Numerical and experimental investigation of thermal convection for a thermodependent Herschel-Bulkley fluid in a annular duct with rotating inner cyclinder. Eur J Mech B 17:875-900

Osunde, O. and Kuru, E. (2008) Open. Fuel. Energy. Sci. J., 1: 19–33 Okon et al. Pressure drop-flow rate profile of some locally formulated drilling fluids using Bingham plastic and power law rheological models, Indian journal of engineering, 2013, 5(12), 10-17

Sifferman TR, Becker TR (1992) Hole cleaning in full-scale inclined wellbores. SPE Drill Eng 7(2):115–120

Turian.R.M.,M.,T.W.,Hs,F,-LG.,Sung,D,-J.,1998 Flow of concentrated Non-Newtonion slurries: 1 Friction losses in laminar, turbulent, transition flow through straight pipe,Int Multiphase Flow 24,225-242

Xiaofeng.S, Kelin.W, Tie.Y, Shuai.S, Jianjun.J, (2014) Effects of drill pipe rotation on cuttings transport using computational fluid dynamics (CFD) in complex structure wells. Springer.comScience,

APPENDICES

Table A-1: Summary of governing equations

Model	Equation
Power law	$\tau = K\dot{\gamma}^n$
Hershel Buckley	$\tau = \tau_0 + k(\dot{\gamma})^n$
Modified Hershel Buckley	$\tau = (1 - exp\left(-\frac{\eta_0 \gamma}{\tau_0}\right))(\tau_0 + k\gamma^n)$
Cross	$\frac{\mu_0 - \mu_\infty}{\mu - \mu_\infty} = 1 + K_{CR}\dot{\gamma} n_{cr}$
Sisko	$\eta = \eta_\infty + \kappa_o \dot{\gamma}^{\eta_o - 1}$

Table A-2: Summary of reported observations

Parameter	Reported Observation	Source
Pressure loss and velocity	Pressure loss more significant under turbulent flow using power law model at drill pipe annulus	Udo and ukon 2013
Drill pipe rotations	The smaller cuttings are easier to transport by increase the rotation speeds with high mud viscosity. In incline well, low viscosity more prefered but depend on cutting size and rotary level.	Sanchez.et.al,2009
Drill pipe eccentricity	When particle velocity increase, it will affect the low annular flow rates at low eccentricity. When eccentricity increase, the rotation speed varies. The effect almost negligible.	Ridchard.et.al,1989

Table A-3: Summary of reported observations

Parameter	Case 1 (Nouar.et al,1998)	Case 2 (Escudier.et al,2002)
Pipe inner diameter(d_i) (mm)	40	50.8
Pipe outer diameter (d_o) (mm)	65	100.4
Pipe length (L) (mm)	165	150.6
Eccentricity	No	Yes

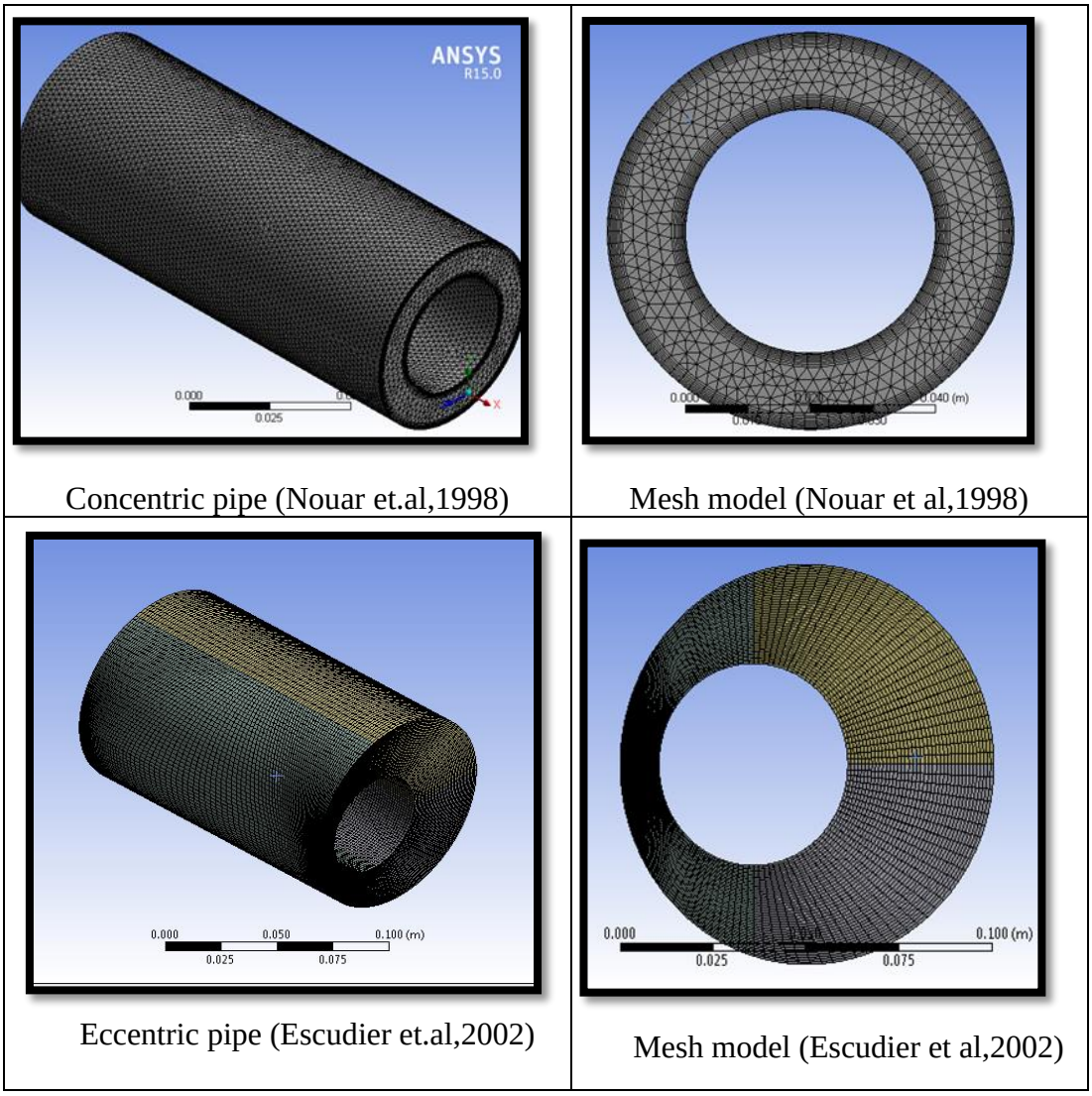

Concentric pipe (Nouar et.al,1998)

Mesh model (Nouar et al,1998)

Eccentric pipe (Escudier et.al,2002)

Mesh model (Escudier et al,2002)

Figure A-1: Isometric view and meshing model

Table A-5: Variables required for CFD simulations (Sun et.al 2014)

No	Groups	Inclination (°)	Flow rate (L/S)	Pipe rotation speed (RPM)
1	1-9	45	30	80,100,120,140,160,180,200,220,240
2	10-18	45	40	80,100,120,140,160,180,200,220,240
3	19-27	45	50	80,100,120,140,160,180,200,220,240
4	28-36	60	30	80,100,120,140,160,180,200,220,240
5	37-45	60	40	80,100,120,140,160,180,200,220,240
6	46-54	60	50	80,100,120,140,160,180,200,220,240
7	55-63	75	30	80,100,120,140,160,180,200,220,240
8	64-72	75	40	80,100,120,140,160,180,200,220,240
9	73-81	75	50	80,100,120,140,160,180,200,220,240
10	82-90	90	30	80,100,120,140,160,180,200,220,240
11	91-99	90	40	80,100,120,140,160,180,200,220,240
12	100-108	90	50	80,100,120,140,160,180,200,220,240

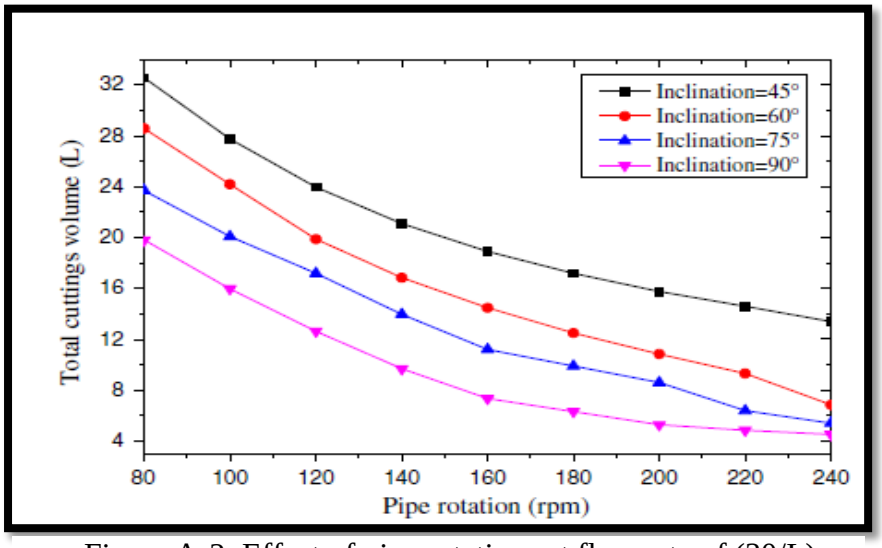

Figure A-2: Effect of pipe rotations at flow rate of (30/L)

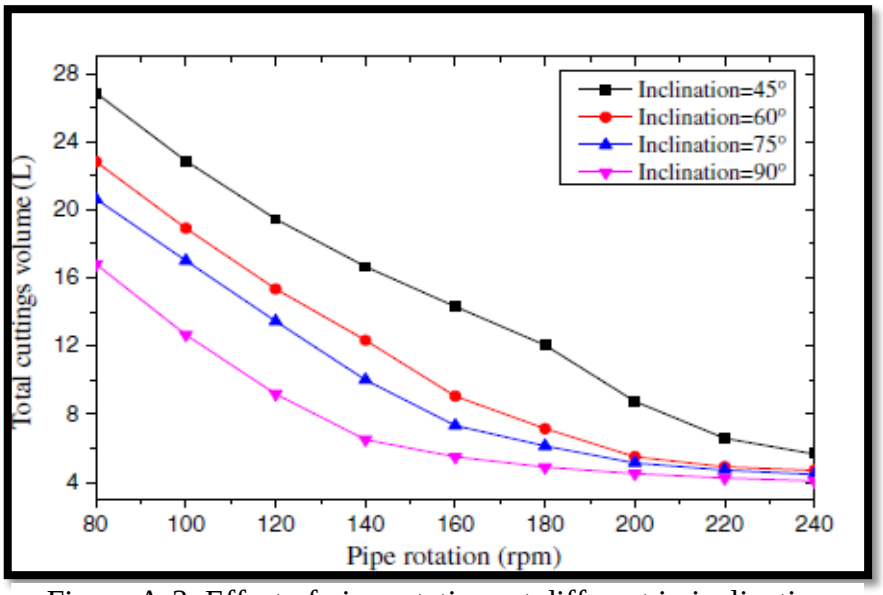

Figure A-3: Effect of pipe rotations at different in inclination angle at flow rate of (40/L)

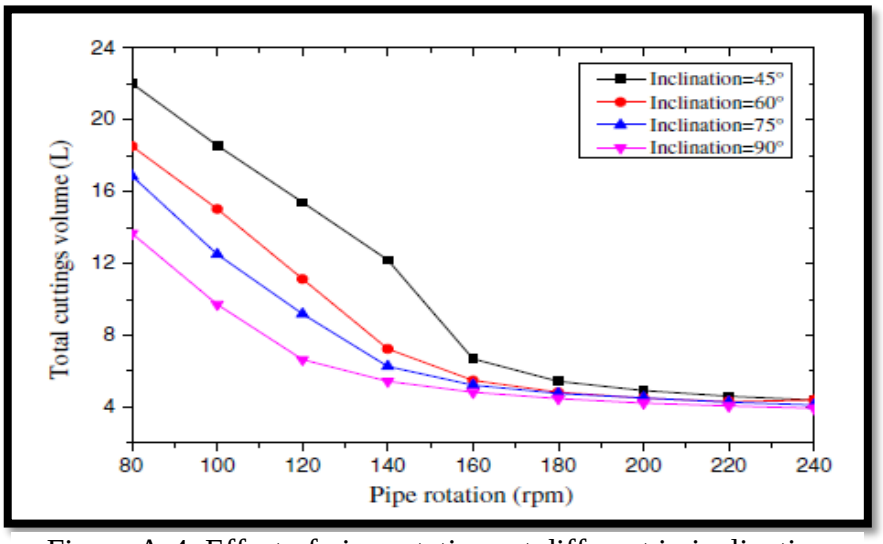

Figure A-4: Effect of pipe rotations at different in inclination angle at flow rate of (50/L)

Table A-6: Input parameter for An OBM mud with an eccentric pipe

Parameter	**Lower limit**	**Upper Limit**
Inlet velocity, (V_{in}, m/s)	0.198	4.902
Rotation, ($\omega, rad/s$)	1.182	14.718
Eccentricity,(ϵ)	0.117	0.993
Theta (θ)	0	85

Table A-7: Rheological parameters of the drilling fluids studied, as a function of OC concentration and pressure for an OBM mud.

$k = k_0 + k_1 \Delta P$		$n = n_0 + n_1 \Delta P$		η_∞ (Pa s)	β (bar^{-1})	AARD (%)
% wt.	k_0 (Pa s^n)	k_1 (Pa s^n bar^{-1})	n_0	n_1 (bar^{-1})		
B128						
1	0.17	$-6.9E-5$	0.65	$1.2E-5$	0.100	0.0027
3	1.27	$-6.8E-4$	0.16	$3.4E-5$	0.153	0.0027
5	**9.55**	**$-1.1E-2$**	**0.09**	**$5.6E-5$**	**0.195**	**0.0028**
B34						
1	0.0081	$1.0E-4$	0.65	$-9.5E-4$	0.118	0.0027
3	0.097	$6.3E-4$	0.55	$-9.4E-4$	0.129	0.0027
5	0.14	$4.7E-4$	0.36	$-3.9E-4$	0.163	0.0027
					0.114	0.0027

**Note: where η is the apparent viscosity, $\eta_{\infty 0}$ is the high-shear-rate-limiting viscosity, k_o the consistency index, and n_o the flow index*

Table A-8: Design of Experiment points for OBM mud analysis

Vin (m/s)	w (rad/s)	e	Offset (mm)	Theta(°)	Dp/dx
2.55	6.822	0.151	1.4345	39.1	-3996
3.334	10.77	0.661	6.2795	35.7	-6757.2
0.198	7.95	0.797	7.5715	15.3	-3456.4
2.942	14.154	0.559	5.3105	32.3	-5110.6
0.59	3.438	0.321	3.0495	66.3	-175.8
4.706	9.642	0.287	2.7265	73.1	-4011
2.746	11.334	0.695	6.6025	69.7	-4709.28
4.51	4.566	0.593	5.6335	42.5	-11800.8
1.57	11.898	0.355	3.3725	59.5	-1471.2
1.178	4.002	0.933	8.8635	83.3	-1926
1.962	2.31	0.117	1.1115	5.1	-2172.6
0.982	13.59	0.491	4.6645	45.9	-545.2
2.354	13.026	0.389	3.6955	25.5	-3257.2
3.53	6.258	0.831	7.8945	8.5	-8639.24
1.766	14.718	0.253	2.4035	76.5	-1873.22
4.118	5.694	0.729	6.9255	28.9	-11381.2
3.922	5.13	0.457	4.3415	79.9	-9266.6
3.138	8.514	0.865	8.2175	11.9	-2135.1
0.786	1.746	0.423	4.0185	18.7	-315.2
0.394	10.206	0.899	8.5405	22.1	-2412.4
2.158	9.078	0.627	5.9565	62.9	-2800.6
4.314	12.462	0.185	1.7575	1.7	-11619.4
4.902	7.386	0.763	7.2485	49.3	-14374.4
1.374	2.874	0.219	2.0805	56.1	-1049.8
3.726	1.182	0.525	4.9875	52.7	-8344.4